Hindawi
Geofluids
Volume 2021, Article ID 5144920, 24 pages
https://doi.org/10.1155/2021/5144920

Research Article

Performance Analysis of Gas Wells Based on the Conventional Decline Parameters and the Flow Integral Equation

Lixia Zhang,[1] **Yong Li**,[1] **Xinmin Song**,[1] **Mingxian Wang**,[2] **Yang Yu**,[1] **Yingxu He**,[3] **and Zeqi Zhao**[1]

[1]*Research Institute of Petroleum Exploration and Development, PetroChina, Beijing 100083, China*
[2]*School of Earth Science and Engineering, Xi'an Shiyou University, Xi'an, Shaanxi 710065, China*
[3]*Bohai Oilfield Research Institute, Tianjin Branch of CNOOC (China) Limited, Tianjin 300459, China*

Correspondence should be addressed to Lixia Zhang; zlx18101302186@126.com

Received 17 September 2021; Accepted 15 November 2021; Published 16 December 2021

Academic Editor: Zhiyuan Wang

The estimation of reserves and performance prediction are two vital tasks for the development of gas reservoirs where the evaluation of gas in place or well-controlled reserves, as the foundation of the performance analysis of gas wells, turns to be exceedingly significant. Advanced production data analysis or modern rate transient analysis (RTA) methods mainly depend on the iterative calculations of material balance quasitime (t_{ca}) and type curve fitting, the essence of which is to update the average reservoir pressure data time and again. The traditional Arps' decline models are of empirical nature despite the convenience and applicability to the constant bottomhole pressure (BHP) condition. In order to avoid the implicit iteration, this paper develops an explicit method for estimating the average reservoir pressure on the basis of dynamic material balance equation (DMBE), termed "flow integral method," which can be applied to various gas production systems under boundary-dominated flow (BDF). Based on the flow integral method and the decline parameter evaluation, we employ the hyperbolic decline model to model the gas well performance at a constant BHP. The analytical formulations of decline rate and decline exponent are deduced from the DMBE and the static material balance equation (SMBE) considering the elastic compressibilities of rock pore and bound water. The resulting decline parameter method for explicit estimation of gas reserves boasts a solid and rigorous theory foundation that production rate, decline rate, and average reservoir pressure profiles have reference to each other, and its implementation steps are explained in the paper. The SMBE can, combined with the estimated pressure profile by the flow integral method, also be used to determine gas reserves which is not limited to the constant-BHP condition and can calibrate the estimates of the decline parameter method. The proposed methods are proven effective and reliable with several numerical cases at different BHPs and a field example.

1. Introduction

The production performance analysis of gas wells runs through the gas reservoir development. The variations of production rate, bottomhole pressure (BHP), cumulative gas production, and average reservoir pressure with time are the basic data for reservoir engineers to implement the analysis and prediction of gas well performance, among which measurements of average reservoir pressure, nonetheless, are far from easy. Therefore, the static material balance relationship (g vs. p_{ave}) is generally used to correlate the average reservoir pressure p_{ave} with the cumulative gas production G_p by the use of reserves G. The determination of average reservoir pressure, from a certain perspective, is equivalent to the determination of gas reserves. The ways of estimating gas in place or gas reserves [1–3] mainly include analogy, volumetric method, material balance analysis, pressure transient analysis (PTA), rate transient analysis (RTA), history matching, and numerical simulation. The volumetric method [4–6] is often used in geological modeling of gas reservoirs or gas fields, and the estimated reserves by static data have relatively low accuracy. The traditional material balance method [7–9] is widely used, but it requires a certain number of measurement points of formation

pressure. Nowadays, PTA and RTA have found their extensive applications in determining the well-controlled reserves. Well testing must be carried out to obtain the accurate pressure data requisite for PTA [10–12] at the expense of production. The daily production data necessary for RTA [13–15], however, are convenient to glean and are analyzed by rigorous theoretical models for which these cost-effective methods have developed rapidly in recent years.

The research on RTA can be traced back to the statistical law of rate data of oil and gas wells presented by Arps [16] who empirically summarized the rate-time relationship into three decline types, namely, exponential, hyperbolic, and harmonic. The conventional hyperbolic decline model (HDM) as a classical tool to analyze the production data of constant-BHP cases is easy to apply, but its theoretical foundation is not fully reckoned with.

Rate decline analysis came into widespread use during the early 1980s when Fetkovich [17, 18] proved that dimensionless rate q_{dD} against time t_{dD} for decline curve analysis during late BDF is subject to the exponential decline law under the constant-BHP condition. Fetkovich's type curves, composed of the dimensionless curves generated by the analytical solution in the transient flow period and Arps' empirical curves in the BDF stage, have created a new direction of modern decline curve analysis where the analytical solution to unsteady flow model and the log-log plot as used in well test analysis are presented. Fetkovich's approach removes the empiricism of Arps' models, but its application is still confined to the slightly compressible fluid because it reckons without the change in gas properties.

Following Fetkovich's investigation, Carter [19, 20] explained the variations of gas viscosity μ and compressibility C_g with pressure by introducing the product ratio $\lambda\,[\lambda = \mu_i C_{gi}/(\mu C_g)]$ and proposed a new set of type curves for gas reservoir analysis. The approximate drawdown parameter takes into account the effect of initial pressure drawdown on the product of gas viscosity and compressibility which enables Carter's approach to be applied to constant-BHP gas flow systems.

In order to address the influence of the changes in production scenarios on data analysis, Blasingame et al. [21] introduced an idea to analyze the production data for variable rate/variable pressure drop systems by using the time function of constant pressure analog which can be obtained by the constant rate analog (or material balance pseudotime t_{ca}) for variable-rate flow under BDF conditions. This approach, for gas well analysis, entails the iterative calculations of t_{ca} to determine the parameters m_{bdf} and b as shown in Equation (4). After that, Palacio and Blasingame [22] demonstrated that the relation of dimensionless rate q_{dD} vs. dimensionless time t_{dD} for the decline curve analysis during BDF coincides with Arps' harmonic decline model based on the material balance time (or pseudotime) function, and then, a new kind of type curves was developed. The innovation of Blasingame's approach is that it not only considers the changes in fluid properties but also fully explains the variations of production schedules as long as the boundary effect can dominate the fluid flow. In addition, other advanced production decline analysis methods such as the normalized pressure integral method (NPI) [23], Agarwal and Gardner's type curves [24, 25] are also applied to the production data analysis of gas wells. The differences between these approaches and Blasingame's type curves (the most representative RTA method) mainly lie in the plot functions; hence, they, in essence, are all consistent with the BDF solutions [26, 27] whether to place emphasis on pressure analysis or rate analysis.

The type curve analysis approaches need an iterative procedure for the determination of gas reserves or material balance pseudotime before curve fitting and parameter interpretation. In addition to type curve analysis, some researchers also proposed other RTA methods to conduct reserve estimation and performance prediction without curve fitting. Blasingame and Lee [27], for instance, presented an iterative method for the determination of gas in place, termed variable-rate reservoir limit testing (VRRLT) of gas wells, where SMBE and iterations of average reservoir pressure are combined to estimate reserves of the volumetric gas reservoir. Zhang et al. [28] developed the VRRLT for abnormally pressured gas reservoirs by considering the compressibilities of rock pore and bound water in the mathematical model of gas flow and SMBE and proposed the selection strategy of initial iteration value.

Mattar and McNeil [29, 30] put forward the "flowing" material balance procedure only applicable to constant-rate cases. This approach, however, may not apply to gas reservoirs because the variation of gas property parameters (such as viscosity, deviation factor, and compressibility) with pressure is not considered and its theoretical basis is not rigorously demonstrated, too.

Mattar et al. [31, 32] developed the dynamic material balance (DMB) procedure, an extension of the flowing material balance, to cope with the rate fluctuations of the gas well. This approach is derived from the "stabilized flow" solution of the gas flow model and the material balance equation of the volumetric gas reservoir. Mattar's dynamic material balance procedure boasts a much stricter fundamental basis than the previous flowing material balance by the use of pseudovariables to tackle the changes in production rate and gas properties. The dynamic material balance equation (DMBE), afterwards, was strictly deduced by Zhang et al. [33] who extended the DMB to abnormally pressured gas reservoirs by incorporating the compressibility effects of irreducible water and rock into SMBE and the gas flow model. Similarly, SMBE, DMBE, and iterations of material balance pseudotime or average reservoir pressure can be combined to estimate gas reserves where the selection strategy of the initial value can refer to Zhang et al. [28].

The VRRLT and DMB function well without type curve fitting, but they still entail the iterations of material balance pseudotime or average reservoir pressure for determination of reserves in an implicit fashion. In order to avoid the iterative procedure, some researchers began to attempt more direct and explicit approaches for reserve estimation with the unremitting application. Ye and Ayala [34] proposed a method to linearize the gas diffusion equation by using density function (ρ) and pseudotime factor (i.e., depletion-

driven time rescaling factor β). The density function, in reality, ignores the viscosity term in pseudopressure, while the treatment of pseudotime factor is consistent with the traditional definition of pseudotime. They evade the iteration of gas reserves for the first time and use the coincidence of liquid solution and numerical simulation results (or gas well data) in the early stage when changes in gas properties are not obvious to select the dimensionless reservoir radius in liquid-type curves, and then, the differences during BDF are employed to determine the λ and β profiles. An approximate relation of λ to ρ is developed to construct the material balance plot, namely, $\lambda^{1/B}$ vs. G_p, for estimation of reserves where the slope of log-log plot of $\mu \cdot C_g$ vs. ρ is approximately reckoned a constant $-B$. This approach is targeted at the rate-time analysis of the gas well in the volumetric gas reservoir under a constant-BHP specification.

Stumpf and Ayala [35] also presented an explicit method for determining gas in place under constant-BHP conditions by the use of q^{1-n} vs. $G_p{}^*$ straight line based on the hyperbolic window (hyperbolic decline period) identification. They stated that the hyperbolic window only exists in the early period of BDF when the decline exponent n can be considered as a constant determined by the initial pseudopressure drawdown ratio r_{mi} and the integral mean value of α with respect to pseudopressure $m(p)$ so the rate data conform to the hyperbolic decline law. The hyperbolic window can be determined by adjusting the rate and time multipliers via the hyperbolic type curve fitting. This approach, however, seems little easy in terms of the whole analysis process and inapplicable to geopressured gas reservoirs where the elastic influences of irreducible water and rock are not negligible.

Alom et al. [36] proposed a type curve fitting method to analyze production data during BDF by using the modified pseudotime function defined by the cumulative gas production G_p. This approach, similar to Blasingame's type curves in principle, uses polynomials to match the relation of $\mu_i C_{gi}/(\mu C_g)$ to G_p, but in fact, the relationship between $\mu_i C_{gi}/(\mu C_g)$ and time t is hard to determine because the profile of average reservoir pressure p_{ave} and the relation of G_p vs. p_{ave} are unknown.

Zhang et al. [37] developed the material balance-quasipressure approximation condition method for determining gas reserves which combines the material balance condition derived from the material-balance principle with the quasipressure approximation condition obtained by solving the mathematical model of gas flow through porous media. This approach also circumvents the determination of material balance pseudotime and works well for both gas reservoirs with abnormal pressure and those with normal pressure under BDF conditions.

Recently, Wang and Ayala [38] extended the hyperbolic decline model under constant-BHP conditions presented by Stumpf and Ayala [35] to the special variable-BHP condition and deduced the decline exponent n for the volumetric gas reservoir. Following the analysis steps of Stumpf and Ayala, they also employed the type-curve fitting and q^{1-n}~$G_p{}^*$ straight-line relation to implement estimation of reserves. It is worth noting that the ratio of pseudopressure at BHP to that at average reservoir pressure is postulated constant. Under this condition, the hyperbolic decline model can be applied to all data during BDF rather than only the early BDF. These approaches, however, reckoned without the elastic effects of irreducible water and rock. Furthermore, the decline exponent in the hyperbolic decline model (Stumpf and Ayala; Wang and Ayala) is evaluated in terms of variable α on average, that is, n is deemed the integral mean of α with respect to pseudopressure $m(p)$ from BHP to initial pressure, but in reality, α is a function of average reservoir pressure (larger than BHP).

Jongkittinarukorn et al. [39] presented a correlation between production rate, decline rate, and decline exponent that relates q vs. $Dn \cdot [d(\ln \lambda)/dp_D]^{-1}$ curve to reserve estimation, based on the viscosity-compressibility ratio λ defined by Carter [20] and the stabilized gas flow equation proposed by Ansah et al. [40, 41], where p_D, a dimensionless pressure, is defined as $(p/Z)/(p_i/Z_i)$; D denotes decline rate and n is decline exponent. They considered the changes in decline exponent for the volumetric gas reservoir at constant-BHP conditions. The synthetic data for validation, nevertheless, is generated by Ansah et al.'s model which is the rationale of Jongkittinarukorn's approach in the first place.

To sum up, the current rate transient analysis methods can be roughly divided into five categories: (1) traditional Arps' decline curve analysis; (2) Fetkovich's and Carter's type curves for constant-BHP production data analysis; (3) modern decline curve analysis represented by Blasingame's type curves capable of analyzing the production system under variable-rate/variable-BHP conditions; (4) the variable-rate reservoir limits testing [27, 28] and dynamic material balance method [31–33] based on the iterations of material balance pseudotime t_{ca} without the curve fitting; (5) some explicit methods [34, 35] to avoid pseudotime calculations. The first method is simple to use, but the theoretical basis is not rigorous. The second is limited to constant-BHP conditions, and curve fitting is complicated. The third and fourth methods are effective in dealing with the BDF data under various production conditions such as constant rate, constant pressure, and even variable rate/variable pressure, but the repeated iterations on average reservoir pressure or pseudotime are indispensable. The fifth category of methods can accomplish reserve estimation in an iteration-free way which has gradually become a research hotspot in the field of gas reservoir performance analysis; however, their applicability to complicated production schedules and abnormally pressured reservoirs remains to be investigated.

Therefore, taking into consideration the compressibility effects of rock and irreducible water, this article is aimed at exploring the explicit methodologies for determining the average reservoir pressure and reserves of a gas reservoir, presenting the theoretical proof of the applicability of the traditional hyperbolic decline model to the gas well with a constant-BHP specification, and eliminating the empiricism

of HDM and the defect that it fails to estimate gas in place. These methodologies can evade the iteration calculations of t_{ca} or p_{ave} and lay the foundation for the performance analysis of gas wells.

The overall layout of this paper is as follows. Firstly, the variable-flowrate solutions (or correlations between rate and pressure during BDF) are introduced. Secondly, the static material balance equation is introduced to deduce the analytic expressions of decline rate and decline exponent; then, we explain the rationales behind the traditional hyperbolic model to characterize the production decline data of constant-BHP gas well and the fundamentals of the decline parameter method available for reserve estimation. Thirdly, the flow integral method is presented for estimating the average reservoir pressure by a reference point during BDF based on the flow integral equation derived from the DMBE, and the implementation steps of the decline parameter method are described. Then, several case investigations from both simulated and realistic data are presented to demonstrate and validate the proposed methodologies. Finally, the innovations of the article are outlined and the conclusions are drawn.

2. Model Development

2.1. Correlations of Rate vs. Pressure during BDF. To linearize the diffusivity equation of gas flow, it is usually necessary to introduce pseudovariables such as

$$p_p = p_i + \frac{\mu_i Z_i}{p_i}\int_{p_i}^{p}\frac{\xi}{\mu(\xi)Z(\xi)}d\xi, \tag{1}$$

$$t_a = \mu_i C_{ti}\int_0^t \frac{1}{\mu C_t}dt, \tag{2}$$

$$C_t = e^{C_\phi(p-p_i)}\left[C_\phi + (1-S_{wc})C_g + S_{wc}C_w\right], \tag{3}$$

where p_p (Pa) denotes pseudopressure, p_i (Pa) is initial reservoir pressure, μ (Pa·s) represents natural gas viscosity, μ_i (Pa·s) denotes gas viscosity at p_i, Z is gas deviation factor or compressibility factor, Z_i denotes gas compressibility factor at p_i, t (s) is time, t_a (s) denotes pseudotime, C_t (Pa^{-1}) represents system compressibility, C_{ti} (Pa^{-1}) represents system compressibility at p_i, S_{wc} represents irreducible water saturation, C_g (Pa^{-1}) denotes gas compressibility, C_ϕ (Pa^{-1}) is rock compressibility, and C_w (Pa^{-1}) is water compressibility. All the symbols in this paper are explained in international standard units (SI) for convenience.

By solving the mathematical model of gas flow with variable rates for a gas well in the center of a closed reservoir, one obtains the solution of boundary-dominated flow (BDF) represented by

$$\frac{p_{p_i} - p_{p_{wf}}}{q} = \frac{\left(\Delta p_p\right)_{i-wf}}{q} = m_{bdf}\cdot t_{ca} + b, \tag{4}$$

$$m_{bdf} = \frac{2\pi\alpha_t}{\alpha_p}\cdot\frac{B_{gi}}{Ah\phi_i C_{ti}} = \frac{1}{G}\cdot\frac{2\pi\alpha_t}{\alpha_p}\cdot\frac{1-S_{wci}}{C_{ti}}, \tag{5}$$

$$b = \frac{\mu_i B_{gi}}{\alpha_p Kh}\left\{\frac{4{r_{eD}}^4\ln r_{eD} - 3{r_{eD}}^4 + 4{r_{eD}}^2 - 1}{4({r_{eD}}^2-1)^2} + \sum_{i=1}^{m}\frac{q_i - q_{i-1}}{q_m}\cdot\left[\sum_{n=1}^{\infty}\frac{2}{{\lambda_n}^2}\cdot f(t_a,\lambda_n)\right]\right\}, \tag{6}$$

$$f(t_a,\lambda_n) = \frac{e^{-{\lambda_n}^2\cdot\left(\alpha_t K/\phi_i\mu_i C_{ti}{r_w}^2\right)\left(t_a - t_{a,i-1}\right)}{J_1}^2(r_{eD}\lambda_n)}{{J_1}^2(r_{eD}\lambda_n) - {J_1}^2(\lambda_n)}, \tag{7}$$

$$t_{ca} = \frac{\mu_i C_{ti}}{q(t)}\int_0^t \frac{q(t)}{\mu(p_{ave})C_t(p_{ave})}dt, \tag{8}$$

where p_{p_i} or $p_p(p_i)$ (Pa) denotes the pseudopressure at p_i, $p_{p_{wf}}$ (Pa) denotes the pseudopressure at bottomhole pressure (BHP) p_{wf}, and q (m^3/s) is the surface production rate of the gas well; t_{ca} (s) represents material balance pseudotime, m_{bdf} (Pa/m^3) denotes the slope of the $(\Delta p_p)_{i-wf}/q$ vs. t_{ca} straight line, and b ($Pa\cdot s/m^3$) is its intercept which is generally reckoned a constant during BDF; G (m^3) is gas in place or gas reserves; $\alpha_p = 2\pi$ and $\alpha_t = 1$ when the international system of units is used.

The relation of pseudopressure at the average reservoir pressure to pseudopressure at BHP under boundary-dominated flow is subject to the dynamic material balance equation [33] given by

$$p_{p_{ave}} = p_{p_{wf}} + q\cdot b, \tag{9}$$

where p_{ave} (Pa) is the average reservoir pressure, and $p_{p_{ave}}$ (Pa) denotes the pseudopressure at p_{ave}.

According to the definition of pseudopressure, Equation (1), we can rewrite Equation (9) as

$$q = \frac{p_{p_{ave}} - p_{p_{wf}}}{b} = \frac{1}{b}\cdot\frac{\mu_i Z_i}{p_i}\left(\int_{p_i}^{p_{ave}}\frac{\xi}{\mu(\xi)Z(\xi)}d\xi - \int_{p_i}^{p_{wf}}\frac{\xi}{\mu(\xi)Z(\xi)}d\xi\right). \tag{10}$$

Equation (10) has the same variable "b" as Equation (4).

2.2. Conventional Decline Parameters

2.2.1. Decline Rate. Taking the derivative of Equation (10) with respect to time, we have

$$\frac{dq}{dt} = \frac{1}{b}\cdot\frac{\mu_i Z_i}{p_i}\left[\frac{p_{ave}}{\mu(p_{ave})Z(p_{ave})}\cdot\frac{dp_{ave}}{dt} - \frac{p_{wf}}{\mu(p_{wf})Z(p_{wf})}\cdot\frac{dp_{wf}}{dt}\right]. \tag{11}$$

When a gas well operates at a constant BHP, dp_{wf}/dt is equal to 0; then, Equation (11) is transformed into

$$\frac{dq}{dt} = \frac{1}{b} \cdot \frac{\mu_i Z_i}{p_i} \cdot \frac{p_{ave}}{\mu(p_{ave}) Z(p_{ave})} \cdot \frac{dp_{ave}}{dt}. \tag{12}$$

Taking into account the compressibilities of rock pore and bound water, the static material balance equation (SMBE) of gas reservoirs captures the intrinsic relationship between average formation pressure and cumulative gas production, which is given by

$$g(p_{ave}) = \frac{p_i}{Z_i}\left(1 - \frac{G_p}{G}\right), \tag{13}$$

$$g(p) = \frac{p}{Z(p)} \cdot \frac{e^{C_\phi (p - p_i)} - S_{wci} e^{-C_w (p - p_i)}}{1 - S_{wci}}, \tag{14}$$

where $g(p)$ denotes the unified pressure function in the SMBE, Pa; G_p is the cumulative gas production, m^3; and S_{wci} represents the irreducible water saturation at p_i.

Differentiating Equation (13) with respect to t gives

$$\frac{dg(p_{ave})}{dt} = -\frac{p_i}{Z_i G}\frac{dG_p}{dt} = -\frac{p_i}{Z_i G} \cdot q. \tag{15}$$

Differentiating Equation (14) with respect to p yields

$$\frac{dg(p)}{dp} = \frac{C(p)}{1 - S_{wci}} \cdot \frac{p}{Z(p)}, \tag{16}$$

$$C(p) = e^{C_\phi (p - p_i)}\left[C_g(p) + C_\phi\right] + S_{wci} e^{-C_w (p - p_i)}\left[C_w - C_g(p)\right], \tag{17}$$

where $C(p)$ denotes the compressibility function dependent on C_w, C_ϕ, and C_g. Though $C(p)$ defined in Equation (17) is different from $C_t(p)$ defined in Equation (3) in form, they are identical in essence and both can be transformed into $(1 - S_{wc}) \cdot C_g$ when C_w and C_ϕ approximate to 0.

According to the chain rule, the derivative of the average reservoir pressure p_{ave} with respect to time t can be expressed as

$$\frac{dp_{ave}}{dt} = \frac{dp_{ave}}{dg(p_{ave})} \cdot \frac{dg(p_{ave})}{dt} = \left[\left.\frac{dg(p)}{dp}\right|_{p=p_{ave}}\right]^{-1} \cdot \frac{dg(p_{ave})}{dt}. \tag{18}$$

By substituting Equations (15) and (16) into Equation (18), one obtains

$$\frac{dp_{ave}}{dt} = \left[\frac{1 - S_{wci}}{C(p_{ave})} \cdot \frac{Z(p_{ave})}{p_{ave}}\right] \cdot \left(-\frac{p_i}{Z_i G} \cdot q\right). \tag{19}$$

The decline rate D is defined as

$$D = -\frac{1}{q}\frac{dq}{dt}. \tag{20}$$

Substituting Equations (12) and (19) into Equation (20) gives

$$D = \frac{\mu_i (1 - S_{wci})}{b \cdot G} \cdot \frac{1}{\mu(p_{ave}) C(p_{ave})}. \tag{21}$$

Equation (21) shows that the decline rate D dependent upon μC is a function of p_{ave} and decreases with time because $1/\mu C$ continues to fall with the falling formation pressure.

2.2.2. Decline Exponent. The decline exponent n is defined as

$$n = \frac{d\left(D^{-1}\right)}{dt}. \tag{22}$$

Substituting Equation (21) into Equation (22) yields

$$n = \frac{bG}{\mu_i (1 - S_{wci})} \cdot \frac{d[\mu(p_{ave}) C(p_{ave})]}{dp_{ave}} \cdot \frac{dp_{ave}}{dt}. \tag{23}$$

By putting Equation (19) into Equation (23), we obtain

$$n = -\frac{p_i}{\mu_i Z_i} \cdot qb \cdot \frac{d[\mu(p_{ave}) C(p_{ave})]}{dp_p(p_{ave})} \frac{dp_p(p_{ave})}{dp_{ave}} \cdot \left[\frac{1}{C(p_{ave})} \cdot \frac{Z(p_{ave})}{p_{ave}}\right]. \tag{24}$$

From Equation (1), it follows

$$\frac{d\left[p_p(p_{ave})\right]}{dp_{ave}} = \frac{\mu_i Z_i}{p_i} \cdot \frac{p_{ave}}{\mu(p_{ave}) Z(p_{ave})}. \tag{25}$$

Substituting Equations (9) and (25) into Equation (24) gives

$$\begin{aligned} n &= -\frac{d[\mu(p_{ave}) C(p_{ave})]}{dp_p(p_{ave})} \cdot \left[\frac{p_{p_{ave}} - p_{p_{wf}}}{\mu(p_{ave}) C(p_{ave})}\right] \\ &= \left[\frac{d\left[\ln (\mu \cdot C)^{-1}\right]}{d\left(\ln p_p\right)} \cdot \frac{p_p - p_{p_{wf}}}{p_p}\right]\Bigg|_{p=p_{ave}}. \end{aligned} \tag{26}$$

The decline exponent n in Equation (26) is similar to the formulations given by Chen and Teufel [42, 43] and the difference lies in the new compressibility function $C(p)$ in the paper. Equation (26) can be further reduced to

$$n = s(p_{ave}) \cdot \gamma(p_{ave}), \tag{27}$$

$$s(p) = \frac{d}{d\left(\ln p_p\right)}\left(\ln \frac{1}{\mu \cdot C}\right), \tag{28}$$

$$\gamma(p) = \frac{p_p - p_{p_{wf}}}{p_p}, \tag{29}$$

where $s(p)$ denotes the derivative of the logarithm of $1/(\mu \cdot C)$

Table 1: Reservoir and gas properties for numerical cases with normal pressure.

Property parameters	Property values	Property parameters	Property values
Grid	$300 \times 120 \times 1$	h	12 m
ϕ_i	0.18	r_w	0.1 m
K_r	9 mD	ρ_{sc}	0.750146 kg/m^3
K_θ	9 mD	M_g	18 g/mol
K_z	0.9 mD	Z_{sc}	0.997515
S_{wci}	0.22	Z_i	0.896867
dr	1.3 m	C_ϕ	5.462×10^{-4} MPa^{-1}
$d\theta$	3°	C_w	4.178×10^{-4} MPa^{-1}
dz	12 m	μ_w	0.432089 cp
p_i	25 MPa	μ_i	$2.193343823 \times 10^{-2}$ cp
T_i	343.15 K	μ_{sc}	$1.075008625 \times 10^{-2}$ cp
T_{sc}	293.15 K	C_{gi}	$3.152713092 \times 10^{-2}$ MPa^{-1}
p_{sc}	0.101325 MPa	C_{ti}	$2.522927812 \times 10^{-2}$ MPa^{-1}
T_{pc}	201.34 K	B_{gi}	$4.265593097 \times 10^{-3}$ m^3/m^3
p_{pc}	4.60 MPa	V_{pi}	1 032 656 m^3
r_e	390 m	G	188 829 866 m^3

with respect to the logarithm of p_p, and $\gamma(p)$ represents the instantaneous pseudopressure level.

It is found that the decline exponent is the product of s (p_{ave}) and $\gamma(p_{ave})$, all of which are dependent on p_{ave} which decreases with time. With falling p_{ave}, $\gamma(p_{ave})$ falls; however, $s(p_{ave})$ tends to rise as a whole. Therefore, n changes slowly with time during the depletion of formation energy and ultimately approaches 0 when gas production is subject to the exponential decline. An equivalent constant is employed to replace the dynamic decline exponent given the slow change in n, and the hyperbolic decline model is used to match the production data of the gas well at a constant BHP in the paper.

Note that b in Equation (9) is considered a constant in the above derivation process and it indeed holds true for a quite long time during BDF. In fact, the value of b, nevertheless, also varies slightly with time.

2.2.3. Estimation of Gas Reserves. The conventional hyperbolic decline model developed by Arps is delineated by three parameters (q_i, D_i, and n), and the production rate and decline rate are represented by

$$q = q_i \cdot (1 + nD_i \cdot t)^{-1/n}, \tag{30}$$

$$D(t) = \frac{D_i}{1 + nD_i \cdot t}, \tag{31}$$

where q_i denotes the initial gas flowrate during BDF, m^3/s; D_i is the initial decline rate, s^{-1}; and n represents the equivalent decline exponent.

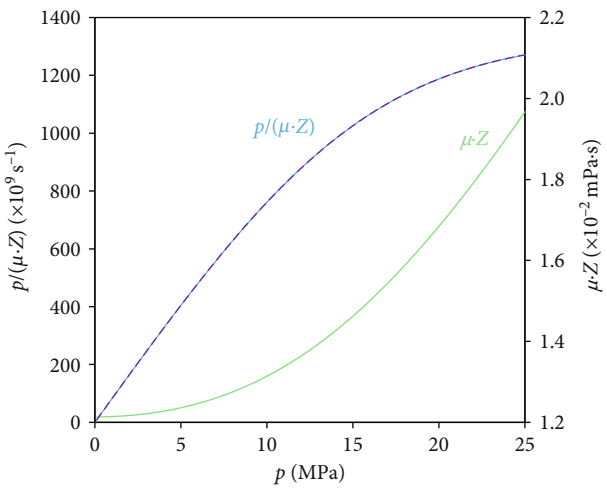

Figure 1: Relation curves of $p/(\mu Z)$ and μZ vs. pressure (p) for the normal pressure cases.

From Equation (21), it follows

$$D_j = \frac{\mu_i(1 - S_{wci})}{b \cdot G} \cdot \frac{1}{\mu\left(p_j\right) C\left(p_j\right)}. \tag{32}$$

According to Equation (10), it follows

$$q_j = \frac{p_p\left(p_j\right) - p_{p_{wf}}}{b}, \tag{33}$$

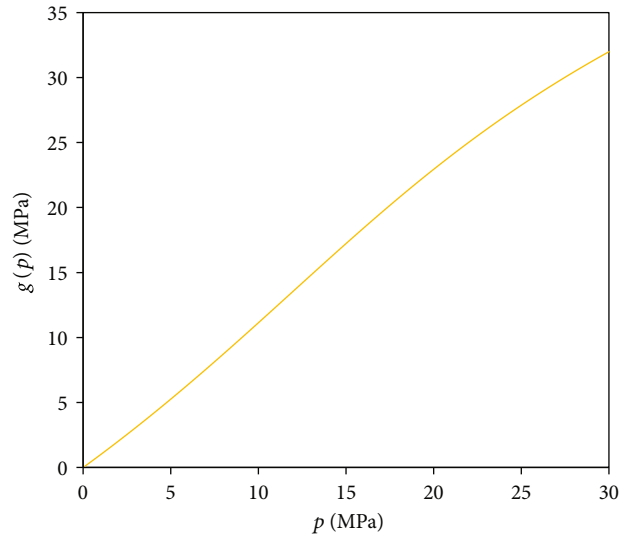

Figure 2: The relation curve of $g(p)$ vs. p for the normal pressure cases.

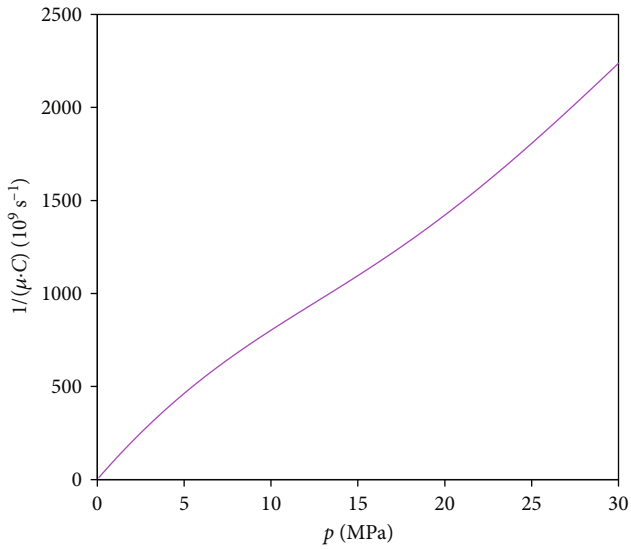

Figure 3: The relation curve of $1/(\mu \cdot C)$ vs. p for the normal pressure cases.

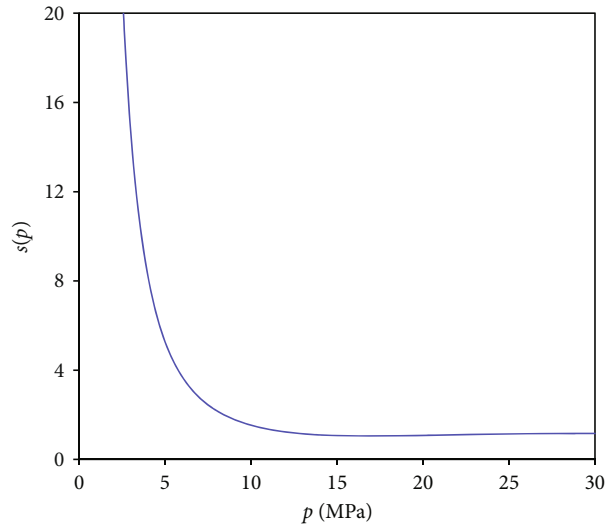

Figure 4: The relation curve of $s(p)$ vs. p for the normal pressure cases.

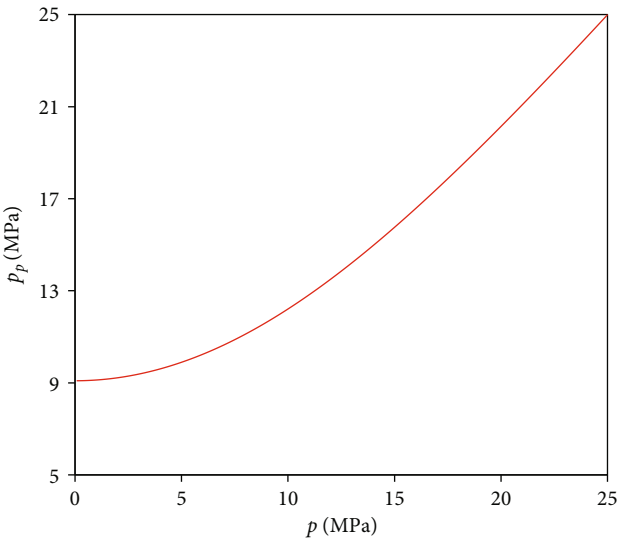

Figure 5: The relation curve of $p_p(p)$ vs. p for the normal pressure cases.

where p_j is the average formation pressure at a certain time t_j, Pa; q_j denotes the production rate at t_j, m^3/s; and D_j is the decline rate at t_j, 1/s.

Based on Equations (32) and (33), q_j/D_j can be written as

$$\frac{D_j}{q_j} = \frac{\mu_i(1 - S_{wci})}{G} \cdot \frac{1}{\mu(p_j)C(p_j)} \cdot \frac{1}{p_p(p_j) - p_{p_{wf}}}. \quad (34)$$

From Equation (34), it follows

$$G_j = \frac{q_j}{D_j} \cdot \frac{\mu_i(1 - S_{wci})}{\mu(p_j)C(p_j)} \cdot \frac{1}{p_p(p_j) - p_{p_{wf}}}, \quad (35)$$

where G_j denotes the calculated reserves from the production data (rate, decline rate, and average reservoir pressure) at t_j, m^3.

Equation (35) reveals that gas reserves can be estimated according to the intrinsic relationship between production rate, decline rate, and average reservoir pressure, but it needs to know the relation of formation pressure to time. Measurements of average reservoir pressure are expensive and time-consuming so it is unrealistic to glean or record the whole profile of p_{ave}. The lack of p_{ave} data prompts us to infer the unknown data points from a limited number of measurement points of average reservoir pressure. What follows in the passage will introduce a method to determine the p_{ave} profile merely based on a certain measurement point during BDF.

Table 2: Production schedules for the numerical cases with normal pressure at constant BHPs.

t (d)	Time step	Δt (h)	Δt (d)	p_{wf} (MPa)
1~2	1~12	1	0.041667	Constant: Case 1-1: 20 Case 1-2: 15 Case 1-3: 10 Case 1-4: 05
	13	3	0.125	
	14	9	0.375	
	15~16	12	0.5	
3~300	17~314	24	1	
301-1100	315~714	48	2	
1101-2000	715~1014	72	3	
2001~3000	1015~1264	96	4	
3001~7000	1265~2064	120	5	

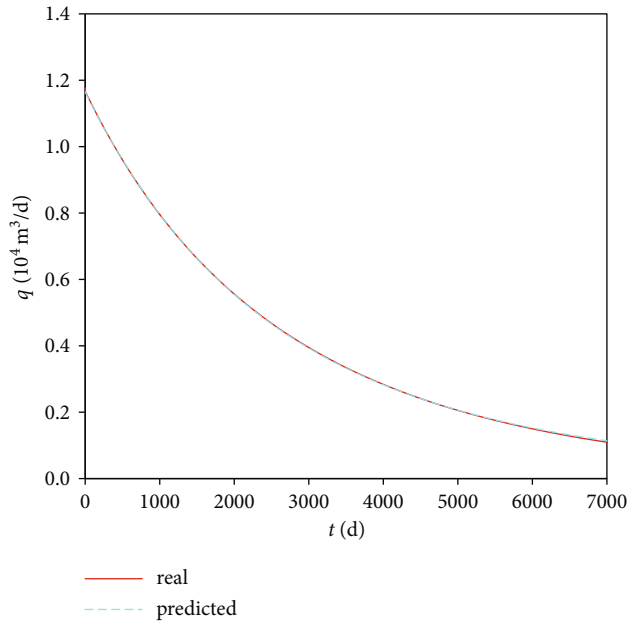

Figure 6: The real production rate profile and the predicted profile by the HDM for Case 1-1.

2.3. The Flow Integral Method for Determination of Average Reservoir Pressure. From Equation (10), it follows

$$q_j = \frac{1}{b} \cdot \frac{\mu_i Z_i}{p_i} \int_{p_{wf,j}}^{p_j} \frac{\xi}{\mu(\xi) Z(\xi)} d\xi. \tag{36}$$

If the formation pressure at t_k is known, then the production rate at that time q_k can be expressed as

$$q_k = \frac{1}{b} \cdot \frac{\mu_i Z_i}{p_i} \int_{p_{wf,k}}^{p_k} \frac{\xi}{\mu(\xi) Z(\xi)} d\xi. \tag{37}$$

Combining Equation (36) with Equation (37), we obtain

$$\int_{p_{wf,j}}^{p_j} \frac{\xi}{\mu(\xi) Z(\xi)} d\xi = \frac{q_j}{q_k} \int_{p_{wf,k}}^{p_k} \frac{\xi}{\mu(\xi) Z(\xi)} d\xi, \tag{38}$$

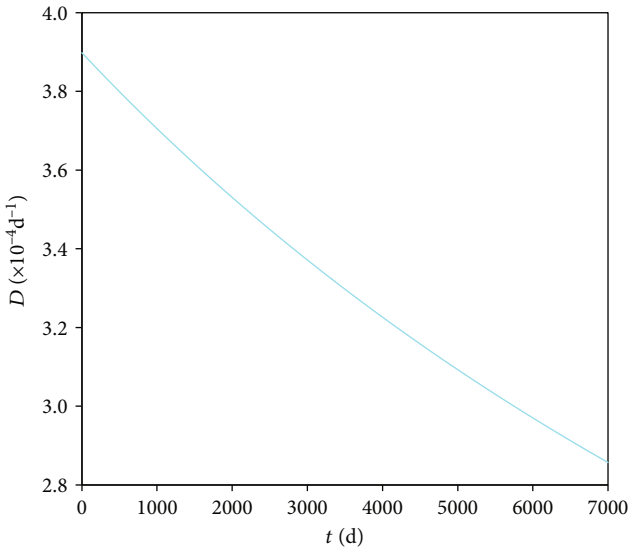

Figure 7: The relation curve of D vs. t for Case 1-1.

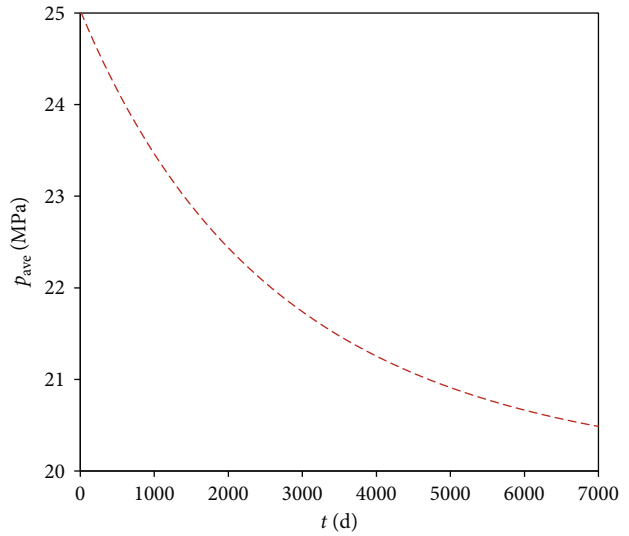

Figure 8: The estimated profile of average reservoir pressure (p_{ave}) for Case 1-1.

where p_k is the average reservoir pressure at t_j, Pa; $p_{wf,k}$ denotes the bottomhole pressure at t_j, Pa.

Equation (38), termed "flow integral equation," indicates that the average reservoir pressure at t_j (i.e., p_j) can be solved by the integral operation of $p/\mu Z$ with respect to p. To speed up the solution process, we utilize the 6th-degree polynomial to approximate the nonlinear function $p/\mu Z$, that is,

$$f_{int}(p) = \frac{p}{\mu(p) Z(p)} \approx a_6 p^6 + a_5 p^5 + a_4 p^4 + a_3 p^3 + a_2 p^2 + a_1 p + a_0. \tag{39}$$

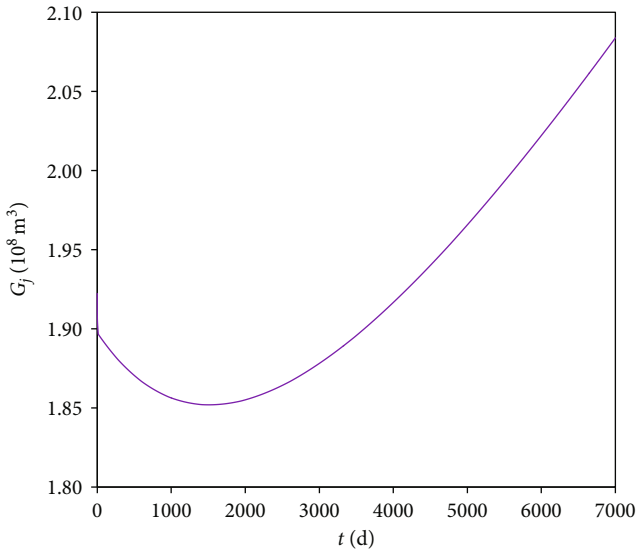

Figure 9: The estimated profile of gas reserves (G_j) for Case 1-1.

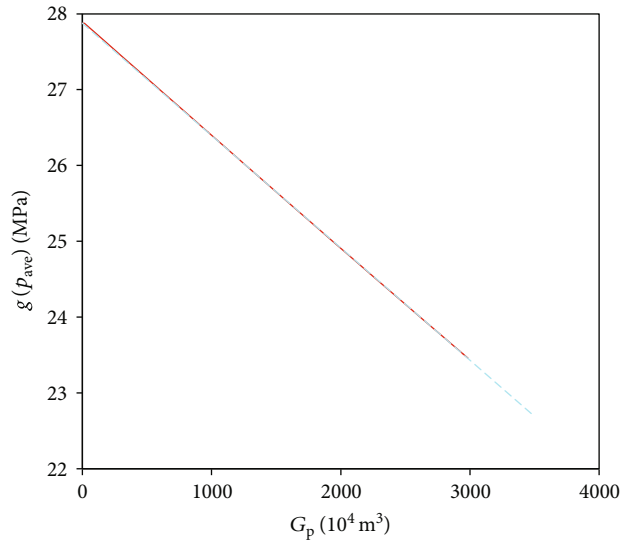

Figure 10: The static material balance relation of $g(p_{ave})$ to G_p for Case 1-1.

From Equation (39), it follows

$$F_{int}(p) = \int \frac{\xi}{\mu(\xi)Z(\xi)} d\xi \approx \frac{a_6}{7}p^7 + \frac{a_5}{6}p^6 + \frac{a_4}{5}p^5 + \frac{a_3}{4}p^4 + \frac{a_2}{3}p^3 + \frac{a_1}{2}p^2 + a_0 p + c, \tag{40}$$

where $F_{int}(p)$ is the antiderivative of $f_{int}(p)$ with respect to p, c is an arbitrary constant (for convenience, let $c = 0$ in the paper), and a_i $(i = 0, 1, 2 \cdots 6)$ denotes the coefficient of the polynomial function used to approximate $p/\mu Z$.

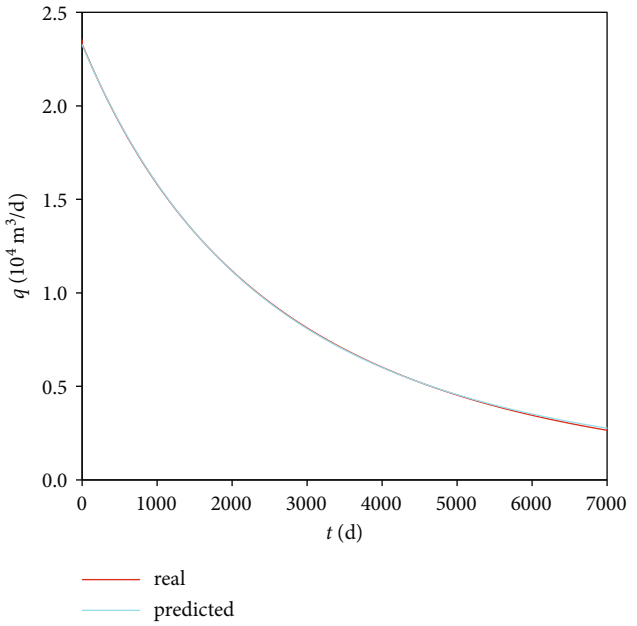

Figure 11: The real q profile and the predicted profile by the hyperbolic decline model for Case 1-2.

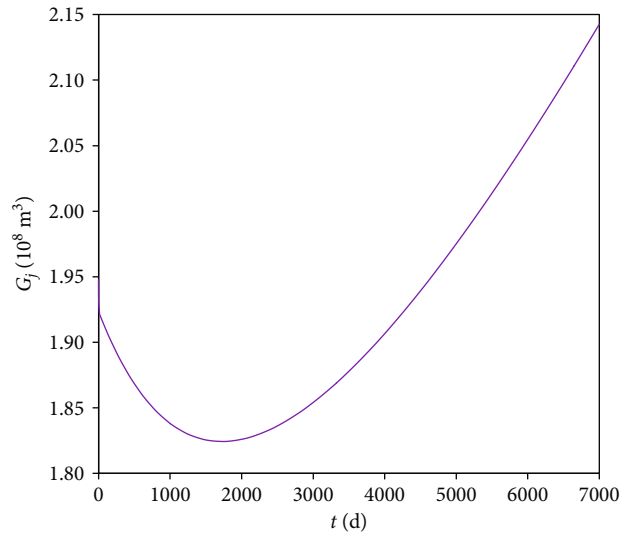

Figure 12: The estimated profile of G_j for Case 1-2.

Substituting Equation (40) into Equation (38), the rearranged equation is represented by

$$F_{int}\left(p_j\right) = \frac{q_j}{q_k}\left[F_{int}(p_k) - F_{int}\left(p_{wf,k}\right)\right] + F_{int}\left(p_{wf,j}\right). \tag{41}$$

Equation (41) is applicable to all cases under BDF, not limited to the constant-BHP condition. If the BHP remains unchanged, then this equation collapses to

$$F_{int}\left(p_j\right) = \frac{q_j}{q_k}\left[F_{int}(p_k) - F_{int}(p_{wf})\right] + F_{int}(p_{wf}). \tag{42}$$

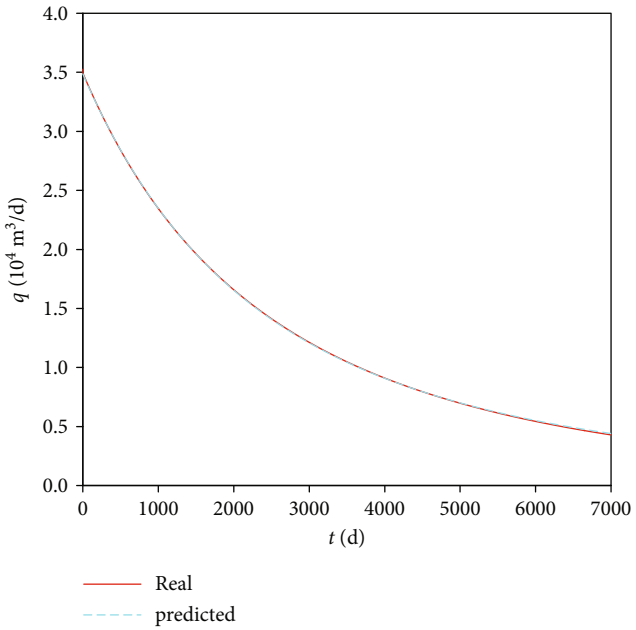

Figure 13: The real q profile and the predicted profile by the hyperbolic decline model for Case 1-3.

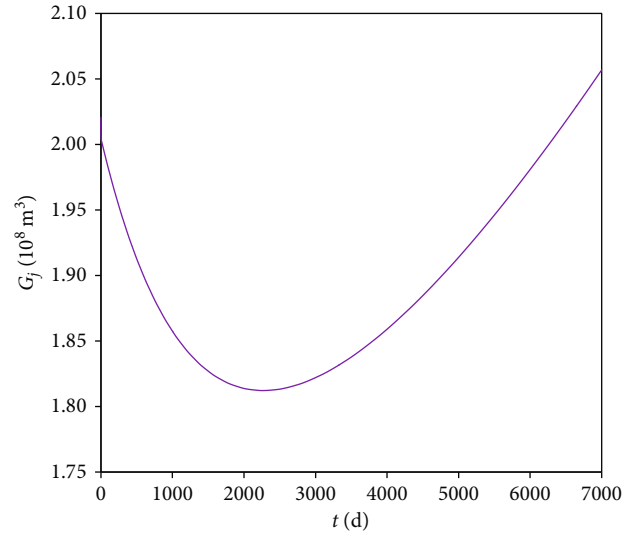

Figure 14: The estimated profile of G_j for Case 1-3.

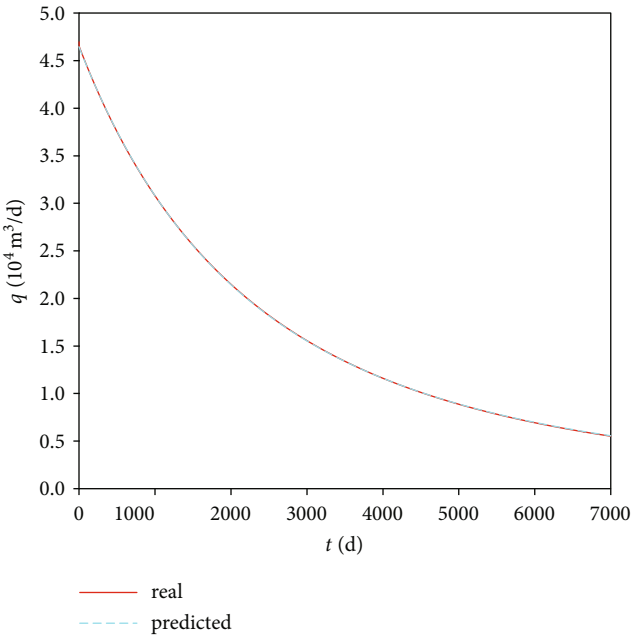

Figure 15: The real q profile and the predicted profile by the hyperbolic decline model for Case 1-4.

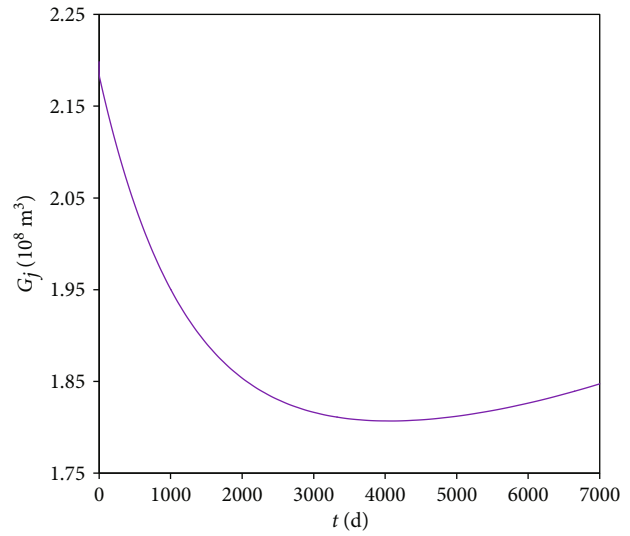

Figure 16: The estimated profile of G_j for Case 1-4.

The right-side terms of Equation (41) are known and its left side is a 7th-degree polynomial; thus, p_j can be easily solved in the range of $p_{\mathrm{wf},j} < p_j < p_{\mathrm{i}}$. The explicit method for estimating the average reservoir pressure data, based on the flow integral equation and one measure point during BDF, is called the "flow integral method" in the paper.

2.4. The Decline Parameter Method for Determination of Gas Reserves. The profile of average reservoir pressure can be determined by the flow integral method so that the terms related to p_{ave} in Equation (35) can also be determined. The profiles of q, D, and p_{ave} can, therefore, be used to conduct the explicit estimation of gas reserves only based on production data. The specific steps are as follows:

(1) Sort out the gas reservoir and fluid property parameters, and determine the multinomial coefficients $a_0 \sim a_6$ in $f_{\mathrm{int}}(p)$

(2) Use the HDM to fit the rate-time data of gas well at a constant BHP and determine three model parameters (q_{i}, D_{i}, and n)

(3) Use Equation (31) to determine the decline rate D

Table 3

(a) The analysis results of the decline parameter method for numerical cases with normal pressure

Normal pressure cases	Case 1-1	Case 1-2	Case 1-3	Case 1-4
p_{wf} (MPa)	20	15	10	5
q_i (10^4 m^3/d)	1.165088	2.326642	3.486867	4.645448
D_i (10^{-4} d^{-1})	3.898168	4.040669	4.217685	4.402959
n	0.133561	0.254215	0.325809	0.331420
G_{HD} (10^8 m^3)	1.907956937	1.906270758	1.897272945	1.915 021414
Error1 (%)	1.041	0.952	0.475	1.415
m (10^{-3} MPa/10^4 m^3)	1.480821926	1.490280824	1.499442534	1.492784717
G_{smb} (10^8 m^3)	1.882387122	1.870439503	1.859010973	1.867302158
Error2 (%)	-0.313	-0.946	-1.551	-1.112

(b) The analysis results of the modified Stumpf method for numerical cases with normal pressure

Normal pressure cases	Case 1-1	Case 1-2	Case 1-3	Case 1-4
p_{wf} (MPa)	20	15	10	5
q_i (10^4 m^3/d)	1.162916	2.319957	3.489227	4.705304
D_i (10^{-4} d^{-1})	3.852920	3.968173	4.228281	4.715305
n_a	0.115682	0.227445	0.325268	0.408158
G_m (10^8 m^3)	1.921676867	1.956024199	1.994686597	2.042141878
Error3 (%)	1.768	3.587	5.634	8.147

(4) Glean the available p_{ave} data and select a certain data point at t_k during BDF to calculate the values of average reservoir pressure with time by the flow integral method

(5) Use q_j, D_j, and p_j to determine G_j based on Equation (35). The average value of G_j is the estimated reserves G_{HD} given by

$$G_{HD} = \frac{1}{N}\sum_{j=1}^{N} G_j, \tag{43}$$

where N denotes the number of data points.

The above iteration-free method, termed the "decline parameter method," can explicitly calculate gas reserves of a constant-BHP system based on the hyperbolic decline parameters and the flow integral equation. The static material balance relationship can be also employed to estimate gas in place after the profile of p_{ave} is obtained by the flow integral method. The intercept of $g(p_{ave})$ vs. G_p straight line is p_i/Z_i, and its slope $-m$ is related to gas reserves G_{smb} defined as

$$G_{smb} = \frac{p_i}{Z_i} \cdot \frac{1}{m}. \tag{44}$$

The value of G_{smb} determined by the SMBE is comparable to G_{HD} estimated by the decline parameter method.

3. Model Validation

In this section, several synthetic cases with different BHPs and a field case are used to illustrate the effectiveness and applicability of the proposed methodologies above. Furthermore, the modified Stumpf method is also introduced for comparison.

3.1. Synthetic Cases: Gas Reservoir with Normal Pressure. A commercial numerical simulator generates the production data of a gas well at constant BHPs centered in a circular reservoir. The simulated gas reservoir has an original pressure (p_i) of 25 MPa, a temperature (T_i) of 70°C (or 343.15 K), and a reference depth of 2500 m. The molar mass of natural gas (M_g) is 18 g/mol, and the pseudocritical temperature and pressure determined by Sutton's correlations [44, 45] are 201.34 K and 4.60 MPa, respectively. Hall and Yarborough's approach [46] is used for calculations of Z-factor and gas compressibility, and Londono et al.'s correlations [47, 48] for gas viscosity. Other property parameters are shown in Table 1.

Figure 1 illustrates the relationships of $p/(\mu \cdot Z)$ vs. p and $\mu \cdot Z$ vs. p for the simulated gas reservoir with normal pressure, and their nonlinearities may result in large error when real pressure or pressure-squared approach is adopted. Equation (45), a 6th-degree polynomial as represented by the dotted line in Figure 1, is used to approximate the relation of $p/(\mu \cdot Z)$ to p, and the polynomial boasts high precision within the range of 0.2 to 25 MPa.

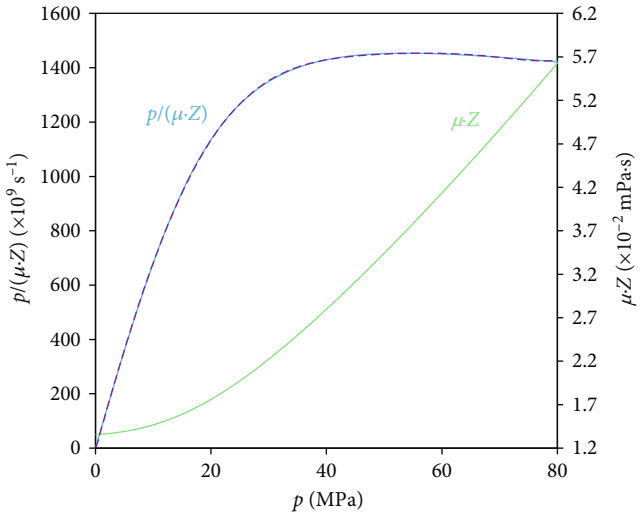

Figure 17: Relation curves of $p/(\mu Z)$ and μZ vs. pressure (p) for the high-pressure cases.

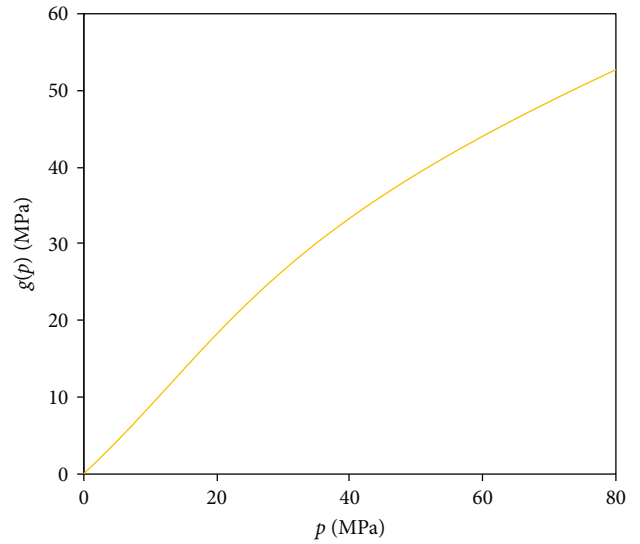

Figure 18: The relation curve of $g(p)$ vs. p for the high-pressure cases.

$$\frac{p}{\mu Z} = -3.854104 \times 10^{-6} p^6 + 2.969799 \times 10^{-4} p^5 - 6.396372 \times 10^{-3} p^4 - 8.938681 \times 10^{-3} p^3 - 1.885397 \times 10^{-1} p^2 + 8.271143 \times 10^{1} p - 1.192612 \times 10^{-1}. \quad (45)$$

The curve of $g(p)$ vs. p shown in Figure 2 reveals the static material balance relationship, and $1/(\mu \cdot C)$ vs. p in Figure 3 reflects the change in the decline rate to some extent. The maximum value of the instantaneous decline exponent $s(p)$ dependent on p is displayed in Figure 4, and the relationship between the pseudopressure p_p and p is shown in Figure 5.

There are 2064 time steps set in the numerical simulation, and the gas well is produced under various constant-

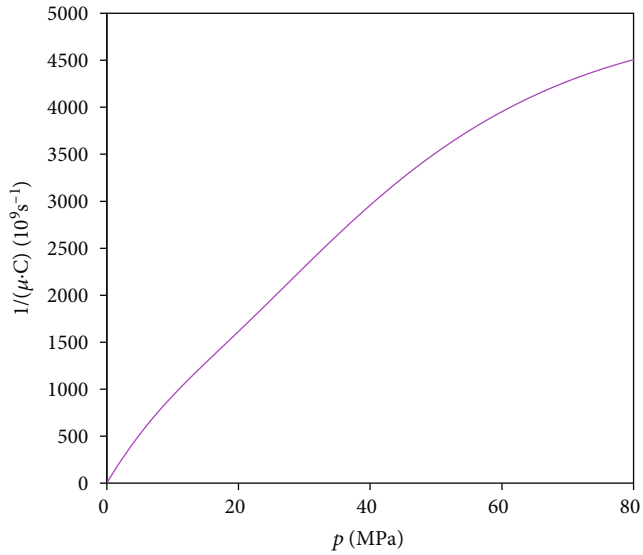

Figure 19: The relation curve of $1/(\mu \cdot C)$ vs. p for the high-pressure cases.

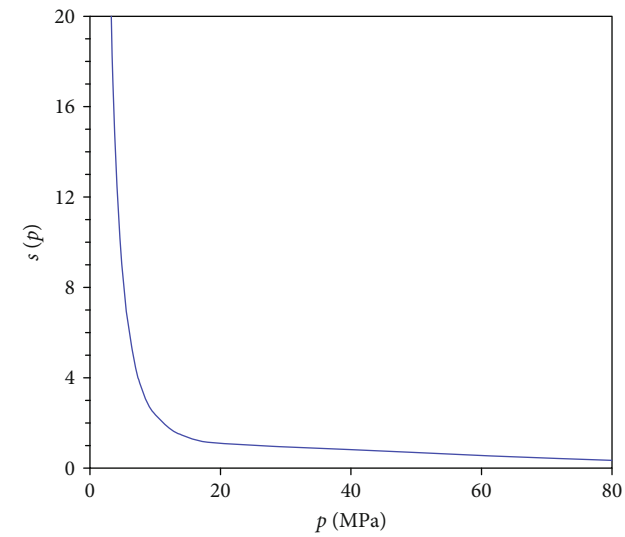

Figure 20: The relation curve of $s(p)$ vs. p for the high-pressure cases.

BHP conditions for 7000 days (about 19.16 years). Four simulated production schedules correspond to four synthetic cases as shown in Table 2.

3.1.1. Case 1-1. The decline parameter method is employed to estimate the gas reserves for Case 1-1 with a BHP of 20 MPa. The solution steps are as follows:

Step 1. Determination of property parameters.

Table 1, Figures 1–5, and Equation (45) display the corresponding results.

Step 2. Determination of hyperbolic decline model.

Equation (30) is used to match the rate-time data of the first 6000 days, and three model parameters are determined as follows: $q_i = 1.165088 \times 10^4$ m^3/d, $D_i = 3.898168 \times 10^{-4}$ d^{-1}, and $n = 0.133561$. The production decline law

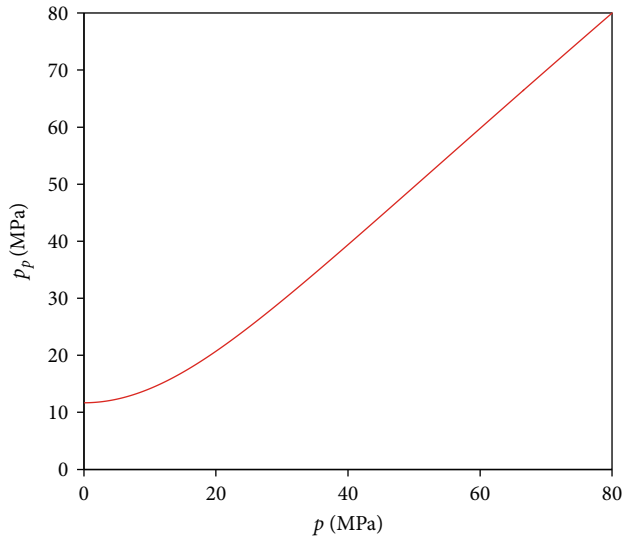

Figure 21: The relation curve of $p_p(p)$ vs. p for the high-pressure cases.

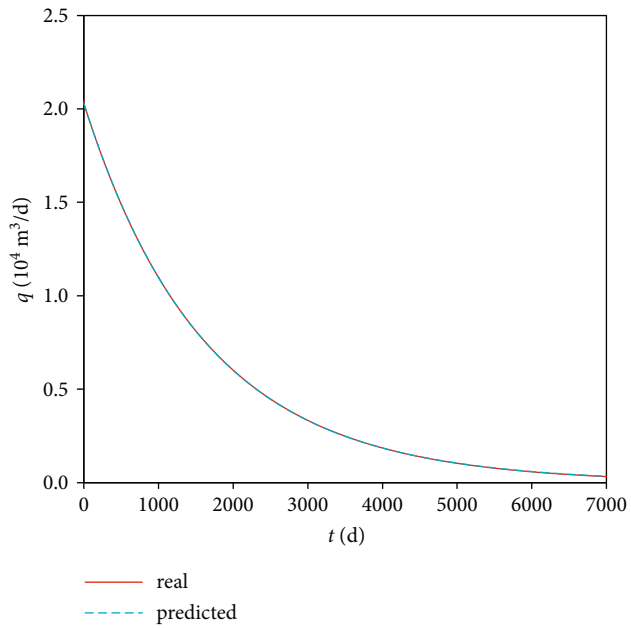

Figure 22: The real q profile and the predicted profile by the HDM for Case 2-1.

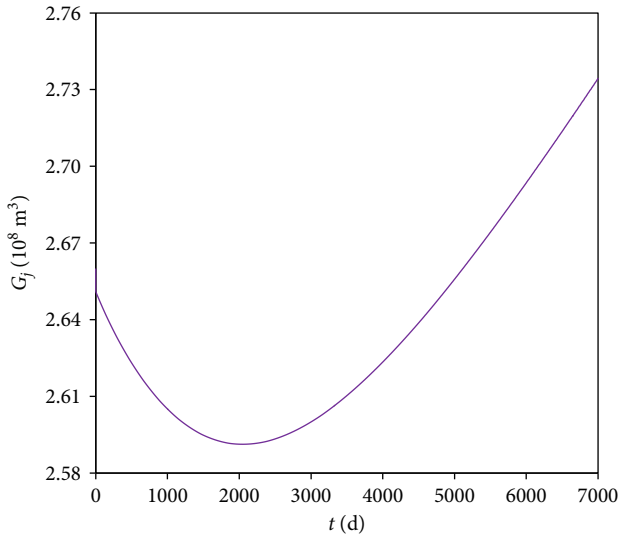

Figure 23: The estimated profile of G_j for Case 2-1.

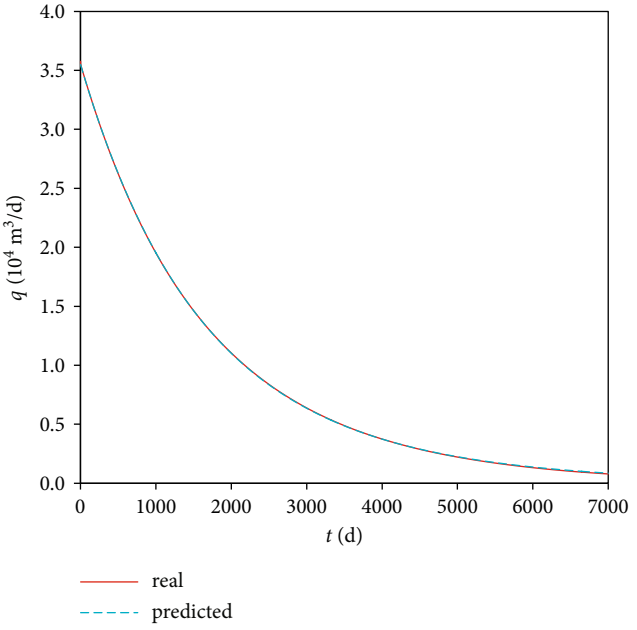

Figure 24: The real q profile and the predicted profile by the hyperbolic decline model for Case 2-2.

characterized by the hyperbolic decline model almost coincides with the actual production rate profile as shown in Figure 6 where an equivalent decline exponent constant could scarcely give rise to large error in the production rate. The instantaneous decline exponent n would approximate to 0 only when the rate q is very low and close to 0 though it varies slowly with time.

Step 3. Calculation of decline rate.

Equation (31) is employed to estimate the corresponding decline rate $D(t)$ at each time point t, as shown in Figure 7.

Step 4. Estimation of average reservoir pressure.

The flow integral method is utilized to determine the average reservoir pressure profile. A reference point is necessary for that method. Take $t_k = 1000$ d as an example here. Equation (42) is adopted to determine the average reservoir pressure at each time point; then, the predicted p_{ave} profile is shown in Figure 8.

Step 5. Estimation of gas reserves.

The value of G_j in Equation (35) can be calculated by the decline rate in Step 3 and the average reservoir pressure in Step 4. Figure 9 shows the profile of estimated reserves, and the resulting G_{HD} is 1.907956937×10^8 m^3 with an error of 1.041%.

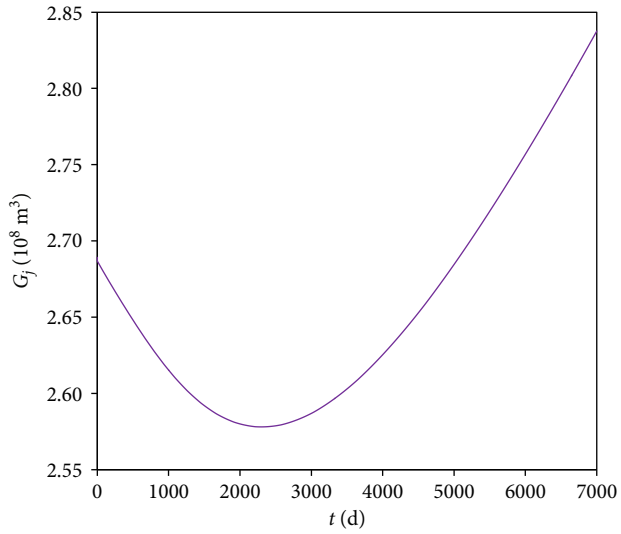

Figure 25: The estimated profile of G_j for Case 2-2.

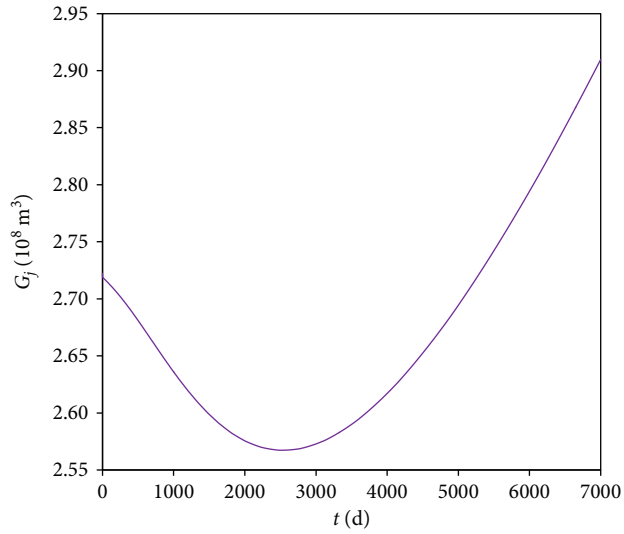

Figure 27: The estimated profile of G_j for Case 2-3.

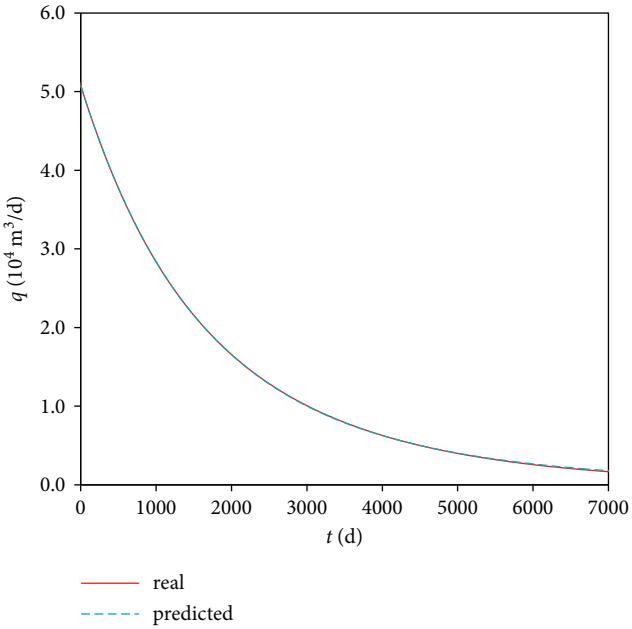

Figure 26: The real q profile and the predicted profile by the hyperbolic decline model for Case 2-3.

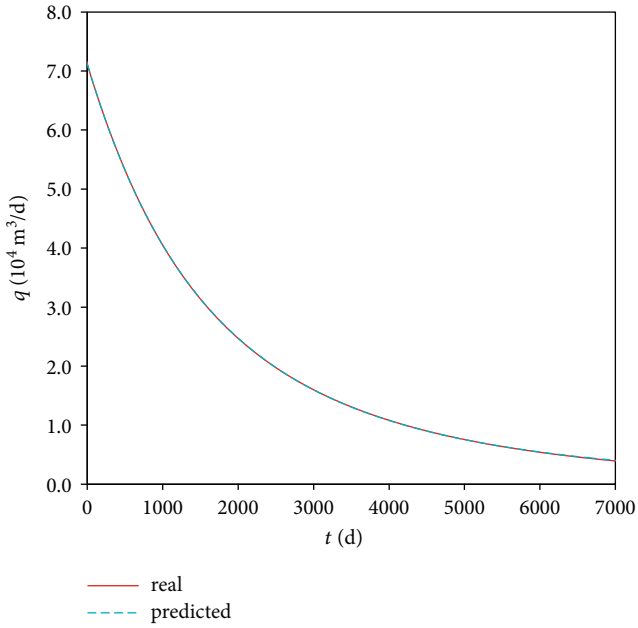

Figure 28: The real q profile and the predicted profile by the hyperbolic decline model for Case 2-4.

Step 6. Verification by the static material balance equation.

The p_{ave} profile in Step 4 can also be used to draw $g(p_{ave})$ vs. G_p curve as shown in Figure 10 where $p_i/Z_i = 27.874801234$ MPa and $-m = -1.480821926 \times 10^{-3}$ MPa/(10^4 m^3). The value of G_{smb} calculated by Equation (44) is 1.882387122×10^8 m^3 with an error of -0.313%. The small difference between G_{smb} and G_{HD} validates the decline parameter method.

3.1.2. Case 1-2. As previously mentioned, Equation (30) is used to match the 6000 d rate profile for Case 2-1 with a constant BHP of 15 MPa, and three model parameters are determined as follows: $q_i = 2.326642 \times 10^4$ m^3/d, $D_i = 4.040669 \times 10^{-4}$ d^{-1}, and $n = 0.254215$. The production rate predicted by the hyperbolic decline model is consistent with the real production profile as shown in Figure 11.

Similarly, take the p_{ave} and q at 1000 d as the reference data. Figure 12 displays the estimated reserve profile, and the resulting value of G_{HD} is 1.906270758×10^8 m^3 with an error of 0.952%. In addition, the straight line of $g(p_{ave})$ vs. G_p has a negative slope $-m$ of $-1.490280824 \times 10^{-3}$ MPa/(10^4 m^3) and G_{smb} determined by the SMBE is 1.870439503×10^8 m^3 with an error of -0.946%.

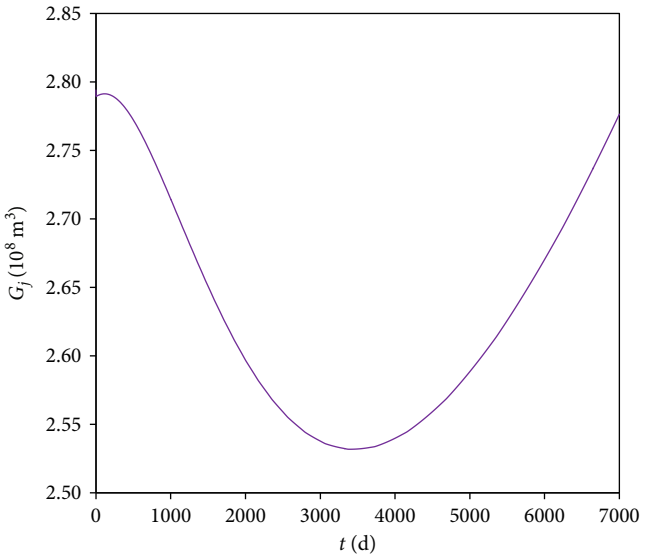

Figure 29: The estimated profile of G_j for Case 2-4.

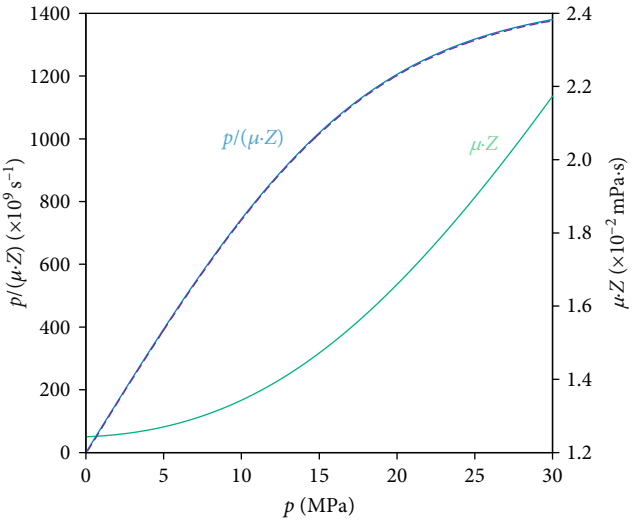

Figure 31: Relation curves of $p/(\mu Z)$ and μZ vs. pressure (p) for Case 3.

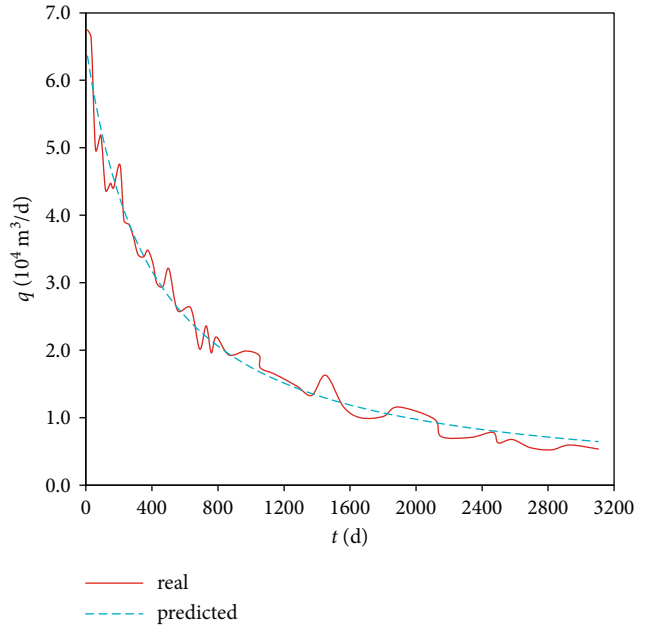

Figure 30: The real q profile and the predicted profile by the hyperbolic decline model for Case 3.

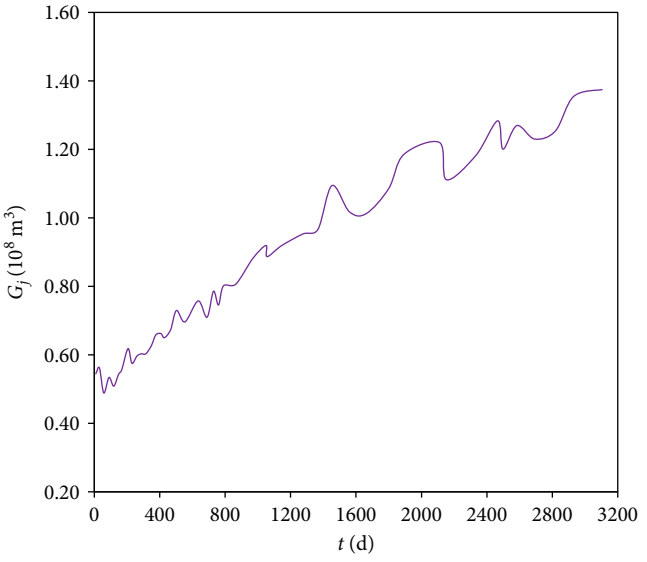

Figure 32: The estimated profile of G_j for Case 3.

3.1.3. Case 1-3. Figure 13 shows the real and predicted profiles of production rate with a BHP of 10 MPa where the dashed line is obtained by the hyperbolic decline model with $q_i = 3.486867 \times 10^4$ m^3/d, $D_i = 4.217685 \times 10^{-4}$ d^{-1}, and $n = 0.325809$. The ultimate G_{HD} of 1.897272945×10^8 m^3 determined by the decline parameter method, as shown in Figure 14, compares favourably with G_{smb} of 1.859010973×10^8 m^3 determined by the SMBE.

3.1.4. Case 1-4. The real and predicted profiles of production rate for Case 1-4 with a BHP of 5 MPa are exhibited in Figure 15 where the dotted line derives from the hyperbolic decline model with $q_i = 4.645448 \times 10^4$ m^3/d, $D_i = 4.402959 \times 10^{-4}$ d^{-1}, and $n = 0.331420$. Figure 16 shows the estimated profile of G_j. Similar to the previous cases, G_{HD} of 1.915021414×10^8 m^3 coincides with G_{smb} of $1.867302158973 \times 10^8$ m^3.

Table 3(a) presents the calculation results of the decline parameter method for the synthetic gas reservoir with normal pressure where Error1 denotes the calculation error of G_{HD} obtained by the decline parameter method and Error2 represents the corresponding error of G_{smb} determined by the static material balance equation.

For the sake of contrast, the modified Stumpf method is developed in the appendix following the research of Stumpf and Ayala [35]. It is necessary for this method to evaluate the average decline exponent (n_a) on the basis of Equations

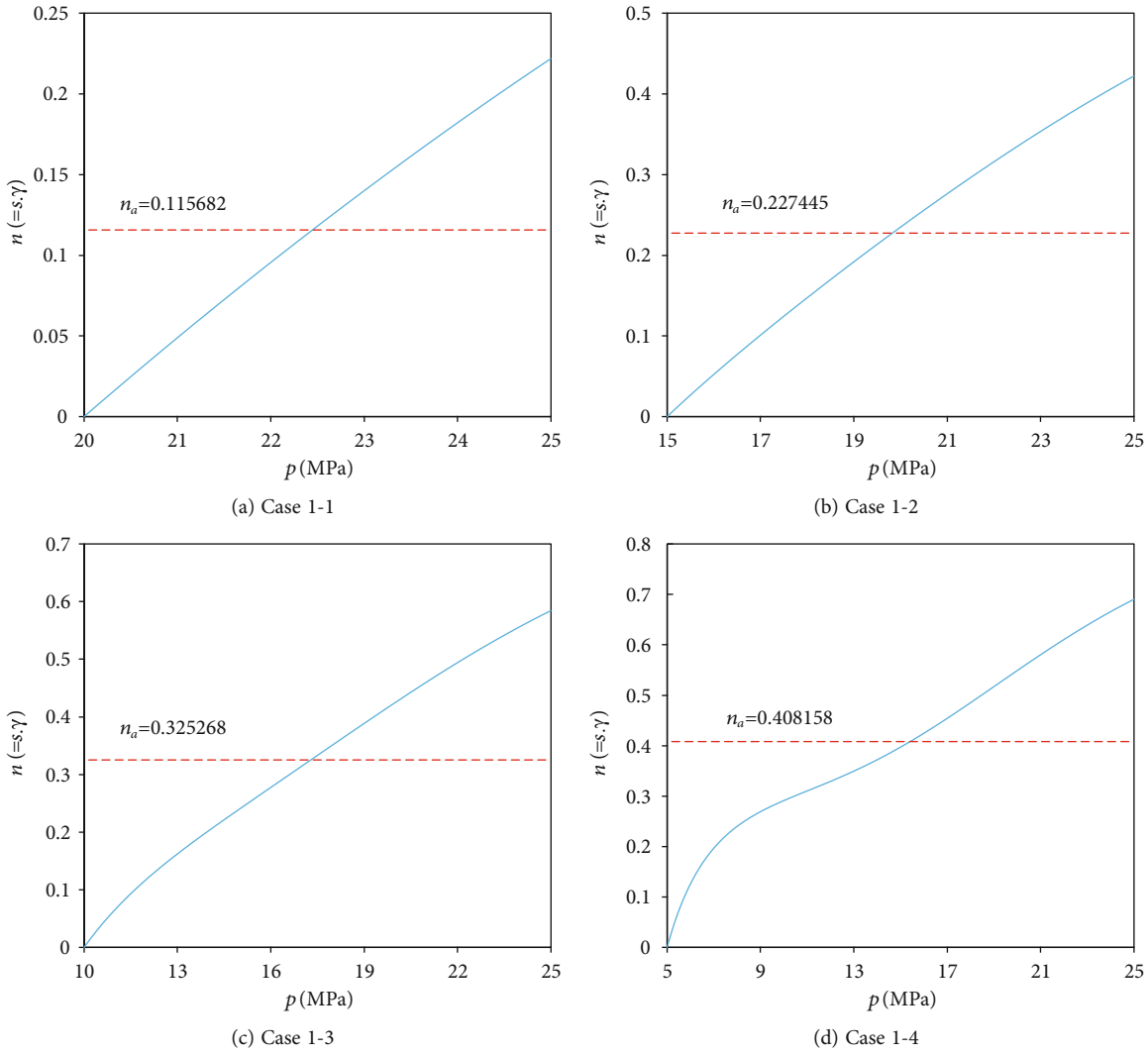

Figure 33: Instantaneous decline exponent n vs. p for the simulated gas reservoir with normal pressure.

(28) and (29); then, the straight line of q^{1-n_a} vs. G_p can be drawn. Its slope and intercept can be used to estimate the decline parameters such as q_i, D_i, and G (see Appendix). The corresponding analysis results for numerical cases with normal pressure are illustrated in Table 3(b) and Figures 33 and 34 (see Appendix), where G_m denotes the value of gas reserves calculated by the modified Stumpf method and Error3 represents its error of estimation.

It can be seen from Tables 3(a) and 3(b) that the decline parameter method provides desirable estimations of gas reserves and decline parameters though the results of the modified Stumpf method are also acceptable except Case 1-4. The differences between two methods lie in the calculation approach of decline exponent and the processing of production data. The former seems more effective in the performance analysis of the relatively low-pressure gas reservoir than the latter which is mainly applicable to early BDF period.

3.2. Synthetic Cases: Gas Reservoir with High Pressure. The gas reservoir with a high initial pressure of 80 MPa is simulated at the temperature of 120°C. Table 4 presents the reservoir and gas properties for the high-pressure cases. Four constant-BHP schedules are generated as shown in Table 5.

Figures 17–21 exhibit the relation curves of $p/(\mu \cdot Z)$ and $\mu \cdot Z$ vs. p, $g(p)$ vs. p, $1/(\mu \cdot C)$ vs. p, $s(p)$ vs. p, and p_p vs. p for the synthetic cases with high pressure, respectively. The nonlinear relationship of $p/(\mu \cdot Z)$ vs. p within the range of $0.2 \le p \le 80$ MPa in Figure 17 can approximately be represented by the following polynomial:

$$\frac{p}{\mu Z} = 7.003288 \times 10^{-8} p^6 - 1.815134 \times 10^{-5} p^5 + 1.719386 \times 10^{-3} p^4 - 6.336605 \times 10^{-2} p^3 - 2.343059 \times 10^{-1} p^2 + 7.586930 \times 10^{1} p - 4.957952. \quad (46)$$

3.2.1. Case 2-1. Figure 22 displays the simulated production profile and the predicted profile by the HDM with three parameters: $q_i = 2.027258 \times 10^4$ m^3/d, $D_i = 6.193329 \times 10^{-4}$ d^{-1}, and

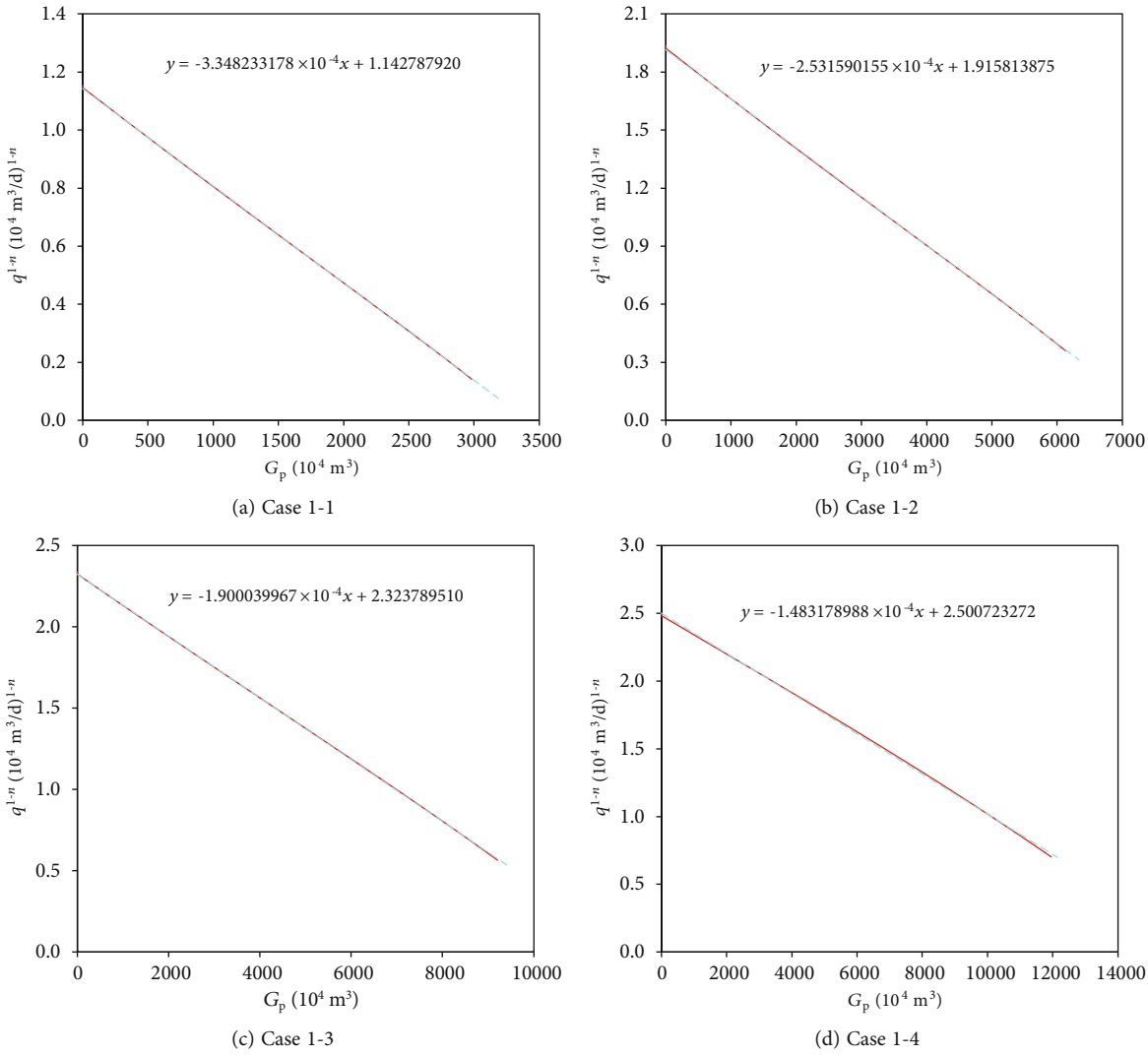

FIGURE 34: q^{1-n} vs. G_p for the simulated gas reservoir with normal pressure.

$n = 0.030078$ for Case 2-1 with a BHP of 64 MPa. The estimated profile of G_j is shown in Figure 23, and G_{HD} is 2.631125906×10^8 m^3. The value of G_{smb} estimated by the SMBE is 2.596071194×10^8 m^3 which compares well with the result of the decline parameter method.

3.2.2. Case 2-2. The real and predicted profiles of production rate for Case 2-2 with a BHP of 52 MPa are illustrated in Figure 24 where the dashed line is obtained by the hyperbolic decline model with $q_i = 3.548\,412 \times 10^4$ m^3/d, $D_i = 6.102\,143 \times 10^{-4}$ d^{-1}, and $n = 0.071877$. Figure 25 shows the estimated profile of G_j determined by Equation (35). Similarly, G_{HD} of 2.650991436×10^8 m^3 coincides with G_{smb} of 2.596831903×10^8 m^3.

3.2.3. Case 2-3. Figure 26 shows the real and predicted profiles of production rate for Case 2-3 with a BHP of 40 MPa in which the dashed line represents the matched hyperbolic decline model with $q_i = 5.073846 \times 10^4$ m^3/d, $D_i = 6.059150 \times 10^{-4}$ d^{-1}, and $n = 0.137588$. Then, the ultimate G_{HD} of 2.667464699×10^8 m^3 determined by the decline parameter method, as shown in Figure 27, is comparable with G_{smb} of 2.596426085×10^8 m^3 determined by the $g(p_{ave})$ vs. G_p curve.

3.2.4. Case 2-4. As mentioned earlier, Equation (30) is used to match the rate profile of the first 6000 days for Case 2-4 with a constant BHP of 24 MPa, and three model parameters are determined as follows: $q_i = 7.120844 \times 10^4$ m^3/d, $D_i = 6.082153 \times 10^{-4}$ d^{-1}, and $n = 0.258\,816$. The production rate predicted by the hyperbolic decline model is in line with the real production profile as shown in Figure 28. The decline parameter method is applied, and Figure 29 displays the estimated reserve profile with the resulting G_{HD} of 2.664141330×10^8 m^3 in line with G_{smb} of 2.596254338×10^8 m^3 determined by the SMBE.

The computation performance of the decline parameter method for the synthetic gas reservoir with high pressure is summarized in Table 6(a). The corresponding analysis results of the modified Stumpf method are displayed in

Table 4: Reservoir and gas properties for numerical cases with high pressure.

Property parameters	Property values	Property parameters	Property values
Grid	$300 \times 120 \times 1$	h	12 m
ϕ_i	0.15	r_w	0.1 m
K_r	5 mD	ρ_{sc}	0.750146 kg/m^3
K_θ	5 mD	M_g	18 g/mol
K_z	0.5 mD	Z_{sc}	0.997515
S_{wci}	0.22	Z_i	1.518784
dr	1.3 m	C_ϕ	1.929×10^{-3} MPa^{-1}
$d\theta$	3°	C_w	4.134×10^{-4} MPa^{-1}
dz	12 m	μ_w	0.235499 cp
p_i	80 MPa	μ_i	$3.705514139 \times 10^{-2}$ cp
T_i	393.15 K	μ_{sc}	$1.075008625 \times 10^{-2}$ cp
T_{sc}	293.15 K	C_{gi}	$5.088279959 \times 10^{-3}$ MPa^{-1}
p_{sc}	0.101325 MPa	C_{ti}	$5.988806368 \times 10^{-3}$ MPa^{-1}
T_{pc}	201.34 K	B_{gi}	$2.586255933 \times 10^{-3}$ m^3/m^3
p_{pc}	4.60 MPa	V_{pi}	860 546 m^3
r_e	390 m	G	259 535 855 m^3

Table 5: Production schedules for the numerical cases with high pressure at constant BHPs.

t (d)	TS	Δt (h)	Δt (d)	p_{wf} (MPa)
1~2	1 ~ 12	1	0.041667	Constant: Case 2-1: 64 Case 2-2: 52 Case 2-3: 40 Case 2-4: 24
	13	3	0.125	
	14	9	0.375	
	15~16	12	0.5	
3~300	17~314	24	1	
301-1100	315~714	48	2	
1101-2000	715~1014	72	3	
2001~3000	1015~1264	96	4	
3001~7000	1265~2064	120	5	

Table 6(b) and Figures 35 and 36 (see Appendix). Two methods both give similar estimations of gas reserves, but the latter shows an increasing error trend with a decrease in p_{wf}.

It is found, from the previous synthetic cases with whether normal pressure or high pressure, that an equivalent decline exponent n is capable of matching the production decline data of the gas well with a constant BHP though the instantaneous decline exponent n as a function of p_{ave} changes slowly with time. The numerical cases fully demonstrate that

(1) The decline parameters of HDM are affected by the BHP of the gas well, and the initial production rate during BDF q_i and the equivalent decline exponent n are more sensitive to BHP values than the initial decline rate D_i. The lower the bottomhole flowing pressure the gas well is produced at, the greater q_i and n are, while the change in D_i is little obvious

(2) The flow integral method, an explicit approach for calculations of average reservoir pressure based on the flow integral equation, can estimate the p_{ave} profile effectively and conveniently because only one data point during BDF is necessary, and in reality, these estimations are not confined to the constant-BHP situations

(3) The decline parameter method, an explicit technique for calculations of gas in place (or gas reserves) based on the conventional decline parameters in HDM can reliably evaluate reserves of the production system with a constant BHP. Furthermore, the value of gas

Table 6

(a) The analysis results of the decline parameter method for numerical cases with high pressure

High-pressure cases	Case 2-1	Case 2-2	Case 2-3	Case 2-4
p_{wf} (MPa)	64	52	40	24
q_i (10^4 m^3/d)	2.027258	3.548412	5.073846	7.120844
D_i (10^{-4} d^{-1})	6.193329	6.102143	6.059150	6.082153
n	0.030078	0.071877	0.137588	0.258816
G_{HD} (10^8 m^3)	2.631125906	2.650991436	2.667464699	2.664141330
Error1 (%)	1.378	2.144	2.778	2.650
m (10^{-3} MPa/10^4 m^3)	2.028978209	2.028383845	2.028700879	2.028835081
G_{smb} (10^8 m^3)	2.596071194	2.596831903	2.596426085	2.596254338
Error2 (%)	0.027	0.057	0.041	0.035

(b) The analysis results of modified Stumpf method for numerical cases with high pressure

High-pressure cases	Case 2-1	Case 2-2	Case 2-3	Case 2-4
p_{wf} (MPa)	64	52	40	24
q_i (10^4 m^3/d)	2.033103	3.563958	5.098227	7.158882
D_i (10^{-4} d^{-1})	6.280879	6.229761	6.194982	6.235047
n_a	0.042862	0.090699	0.157294	0.281530
G_m (10^8 m^3)	2.610138552	2.623031736	2.639488727	2.673866274
Error3 (%)	0.569	1.066	1.700	3.025

reserves calculated by the static material balance equation is available for the mutual verification with the estimate of the decline parameter method

(4) The production data matching in the decline parameter method could be superior to the analytic calculations of q_i, D_i, and n_a in the modified Stumpf method based on the straight line of q^{1-n_a} vs. G_p which is only suitable for early BDF data. The former extends the range of application of the latter. These approaches, however, can be verified against each other

(5) The decline parameter method is valid for both high-pressure and normal pressure gas reservoirs. The calculation errors for the high-pressure system, however, are slightly larger than those of the low-pressure system which may be attributed to the more decrease in formation pressure and a bit severer fluctuation in b during BDF for high-pressure gas reservoirs

3.3. Field Case: Gas Well A in West Virginia. Case 3, a field example provided by Fetkovich et al. [18], reflects the production scenario of *Gas Well A* in West Virginia. Fraim and Wattenbarger [49] also investigated this case and digitized the raw rate-time data as shown in Figure 30. The hyperbolic decline model is used to fit the rate profile, and the resulting three parameters are as follows: $q_i = 6.509603 \times 10^4$ m^3/d, $D_i = 2.534238 \times 10^{-3}$ d^{-1}, and $n = 0.907\,180$.

Since the specific gravity of the natural gas is 0.57, we obtain the pseudocritical temperature T_{pc} and pressure p_{pc} are 191.22 K and 4.61 MPa, respectively, according to Sutton [44, 45]. Other property parameters are shown in Table 7.

As revealed by the dotted line in Figure 31, the relation of $p/(\mu \cdot Z)$ to p for Case 3 can be represented by the following polynomial in the pressure range of 0.2 to 30:

$$\frac{p}{\mu Z} = -1.612592 \times 10^{-6} p^6 + 1.292460 \times 10^{-4} p^5 - 2.355782 \times 10^{-3} p^4 - 3.709335 \times 10^{-2} p^3 - 9.545551 \times 10^{-2} p^2 + 8.033991 \times 10^{1} p + 9.824220 \times 10^{-2}. \quad (47)$$

According to Fetkovich et al., the average reservoir pressure at 200 days is 3268 psi (or 22.532067 MPa), and the corresponding production rate is estimated to be 4.289933×10^4 m^3/d by the matched hyperbolic model. Then, the formation pressure profile is determined by the flow integral method. Figure 32 displays the estimated reserve profile by implementing the above steps of the decline parameter method.

The average value of G_j for Case 3 leads to a G_{HD} of $0.857228\,577 \times 10^8$ m^3; however, G_{smb} is not estimated because of unavailable cumulative production. The negligible difference between G_{HD} in the paper and the estimate for gas in place of $0.303\,451 \times 10^7$ Mscf (or 0.859277542×10^8 m^3) predicted by Fraim and Wattenbarger [49] using normalized time matching demonstrates the applicability and feasibility of the decline parameter method.

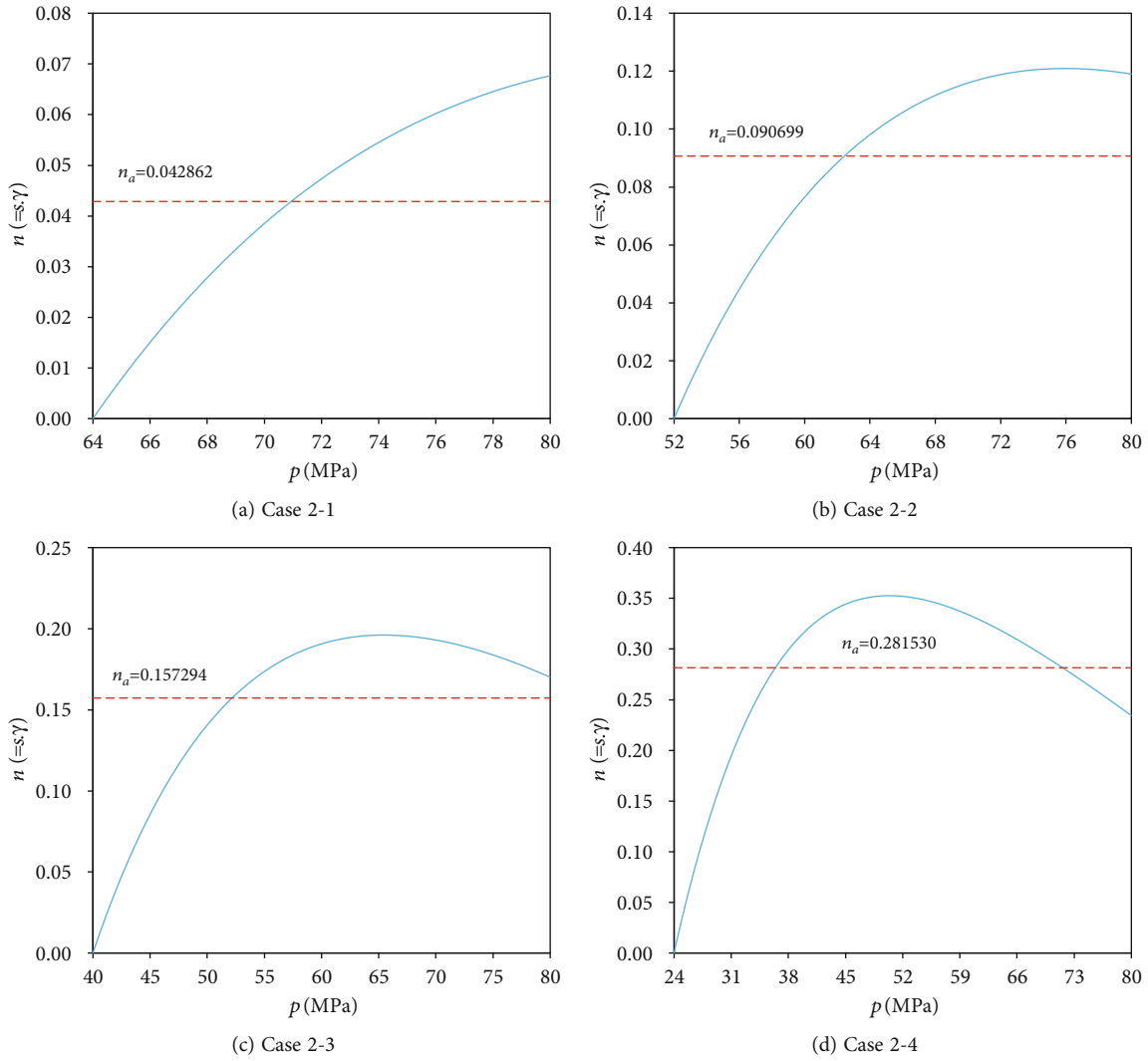

FIGURE 35: Instantaneous decline exponent n vs. p for the simulated gas reservoir with high pressure.

4. Conclusions

The flow integral equation during BDF is derived in the paper from the dynamic material balance equation of the gas reservoir; then, the flow integral method based on it is proposed for explicit determination of the average reservoir pressure profile. The decline parameter method, a novel approach for explicit estimation of gas reserves, is developed to evaluate the reserves of the gas well at a constant BHP on the basis of the conventional hyperbolic decline model and the predicted formation pressure data by the flow integral method; and the static material balance equation, on the other hand, can be used to verify the results. These methods are suitable for both abnormally pressured gas reservoirs and normal pressure systems because the compressibilities of rock and bound water are considered in the rationales. The following conclusions are drawn:

(i) The hyperbolic decline model with a constant decline exponent n can accurately delineate the production rate data of the gas well at a constant BHP, although the actual value n varies slowly with time

(ii) The values of BHP influence the decline parameters (q_i, D_i, and n) in HDM, and the initial decline rate D_i is relatively insensitive to BHPs compared to the other two parameters. The smaller the BHP is, the larger q_i and n are

(iii) The flow integral method, not limited to the constant-BHP conditions, is effective in estimating the profile of average reservoir pressure for various gas production systems during BDF in an explicit fashion

(iv) The decline parameter method, capturing the intrinsic correlation between production rate, decline rate, formation pressure, and gas reserves, is mainly applicable to the production well with a constant BHP and can also provide results of reference for those gas wells with slight fluctuations in BHP

Table 7: Reservoir and gas properties for Case 3.

Property parameters	Property values	Property parameters	Property values
p_i	28.785612 MPa	h	21.336 m
T_i	344.26 K	r_w	0.1079 m
p_{wf}	3.447379 MPa	ρ_{sc}	0.687754 kg/m^3
ϕ_i	0.06	M_g	16.509480 g/mol
S_{wci}	0.35	Z_{sc}	0.997913
T_{sc}	293.15 K	Z_i	0.952170
p_{sc}	0.101325 MPa	μ_i	$2.209414019 \times 10^{-2}$ cp
T_{pc}	191.218772 K	μ_{sc}	$1.100728475 \times 10^{-2}$ cp
p_{pc}	4.605256 MPa	C_{gi}	$2.589484787 \times 10^{-2}$ MPa^{-1}
C_ϕ	8.816×10^{-4} MPa^{-1}	C_{ti}	$1.785752111 \times 10^{-2}$ MPa^{-1}
C_w	4.122×10^{-4} MPa^{-1}	B_{gi}	$3.944216913 \times 10^{-3}$ m^3/m^3

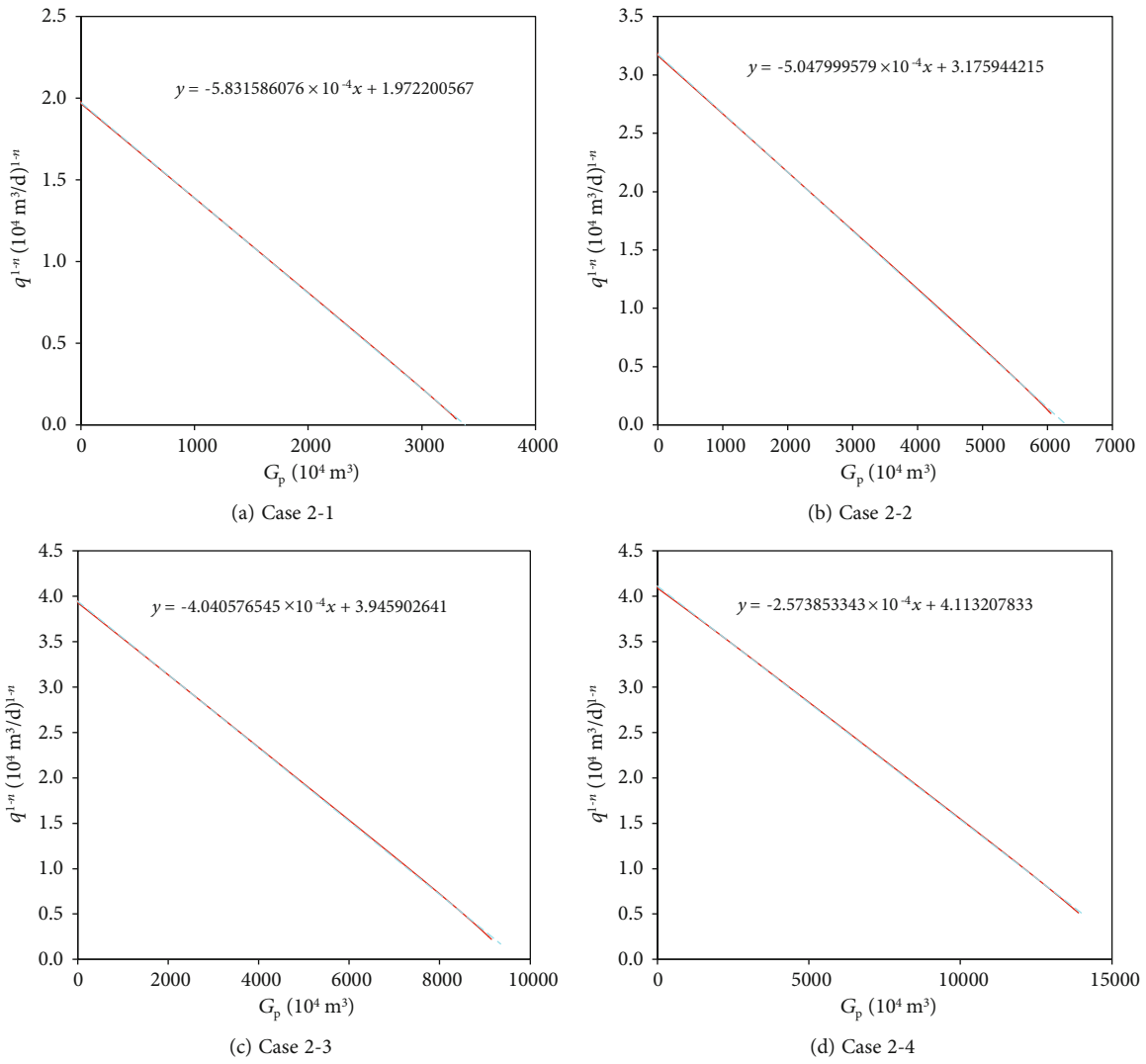

Figure 36: q^{1-n} vs. G_p for the simulated gas reservoir with high pressure.

(v) The production data matching in the decline parameter method could be superior to the analytic calculations of q_i, D_i, and n_a in the modified Stumpf method based on the straight line of q^{1-n_a} vs. G_p which is limited to relatively early BDF period. These approaches, nonetheless, can be verified against each other

(vi) The static material balance equation, combined with the estimated formation pressure data by the flow integral method, is also capable of determining the reserves accurately, which can also be employed to verify the decline parameter method

Appendix

Modified Stumpf Method

Both Stumpf and Ayala [35] and Wang and Ayala [38] used the linear relationship between q^{1-n} and $G_p{}^*$ to determine gas reserves. Considering the different pseudopressure definition in this paper from Stumpf and Ayala and Wang and Ayala, we need to rederive the expressions of initial production rate (q_i), initial decline rate (D_i), pressure-averaged decline exponent (n_a), and gas in place (G).

Similar to the average value of n presented by Stumpf and Ayala, we introduce a pressure-averaged decline exponent (n_a) given by

$$n_a = \frac{1}{\xi_1 - \xi_0}\int_{\xi_0}^{\xi_1} s(\xi)\gamma(\xi)d\xi \approx \frac{1}{p_i - p_{wf}}\int_{p_{wf}}^{p_i} s(\xi)\gamma(\xi)d\xi. \quad (A.1)$$

The relation of cumulative gas production (G_p) to time (t) in the hyperbolic decline model can be written as

$$G_p = \frac{q_i}{(n_a - 1)D_i}\left[(1 + n_a D_i \cdot t)^{(-1/n_a)(1-n_a)} - 1\right] (n_a > 0, n \neq 1). \quad (A.2)$$

Due to

$$\frac{q}{q_i} = (1 + n_a D_i \cdot t)^{-1/n_a}, \quad (A.3)$$

Equation (A.2) is transformed into

$$G_p = \frac{q_i}{(1 - n_a)D_i}\left[1 - \left(\frac{q}{q_i}\right)^{1-n_a}\right]. \quad (A.4)$$

From Equation (A.4), it follows

$$\left(\frac{q}{q_i}\right)^{1-n_a} = 1 - \frac{(1 - n_a)D_i}{q_i}G_p. \quad (A.5)$$

According to Equations (9) and (21), the initial production rate (q_i) and the initial decline rate (D_i) can be expressed as

$$q_i = \frac{p_p(p_{bdf,i}) - p_{p_{wf}}}{b}, \quad (A.6)$$

$$D_i = \frac{\mu_i(1 - S_{wci})}{b \cdot G} \cdot \frac{1}{\mu(p_{bdf,i})C(p_{bdf,i})}, \quad (A.7)$$

where $p_{bdf,i}$ denotes the reservoir pressure at the start of BDF.

Then, D_i/q_i is given by

$$\frac{D_i}{q_i} = \frac{\mu_i(1 - S_{wci})}{G} \cdot \frac{1}{\mu(p_{bdf,i})C(p_{bdf,i})} \cdot \frac{1}{p_p(p_{bdf,i}) - p_{p_{wf}}}. \quad (A.8)$$

Substituting Equation (A.8) into Equation (A.5) gives

$$q^{1-n_a} = q_i{}^{1-n_a} - \frac{\mu_i(1 - S_{wci})}{G} \cdot \frac{1 - n_a}{\mu(p_{bdf,i})C(p_{bdf,i})} \cdot \frac{q_i{}^{1-n_a}}{p_p(p_{bdf,i}) - p_{p_{wf}}}G_p \quad (A.9)$$

We denote the slope and the intercept of q^{1-n_a} vs. G_p straight line by m_h and b_h, respectively, that is,

$$m_h = -\frac{\mu_i(1 - S_{wci})}{G} \cdot \frac{1 - n_a}{\mu(p_{bdf,i})C(p_{bdf,i})} \cdot \frac{q_i{}^{1-n_a}}{p_p(p_{bdf,i}) - p_{p_{wf}}}, \quad (A.10)$$

$$b_h = q_i{}^{1-n_a}. \quad (A.11)$$

So m_h divided by b_h is equal to

$$\frac{m_h}{b_h} = -\frac{\mu_i(1 - S_{wci})}{G} \cdot \frac{1 - n_a}{\mu(p_{bdf,i})C(p_{bdf,i})} \cdot \frac{1}{p_p(p_{bdf,i}) - p_{p_{wf}}}. \quad (A.12)$$

From Equation (A.12), it follows

$$G = -\frac{b_h}{m_h} \cdot \frac{\mu_i(1 - S_{wci})}{\mu(p_{bdf,i})C(p_{bdf,i})} \cdot \frac{1 - n_a}{p_p(p_{bdf,i}) - p_{p_{wf}}}. \quad (A.13)$$

From Equation (A.11), it follows

$$q_i = b_h{}^{1/(1-n_a)}. \quad (A.14)$$

Substituting Equations (A.13) and (A.14) into Equation (A.8) yields

$$D_i = \frac{-m_h}{1 - n_a} \cdot b_h{}^{n_a/(1-n_a)}. \quad (A.15)$$

As Stumpf and Ayala [35] mentioned, $p_{bdf,i}$ approximate to p_i during early BDF, therefore, Equation (A.13) can be rewritten as

$$G \approx -\frac{b_h}{m_h} \cdot \frac{1 - S_{wci}}{C(p_i)} \cdot \frac{1 - n_a}{p_{p_i} - p_{p_{wf}}}. \quad (A.16)$$

The above discussion on decline parameters follows the idea of Stumpf and Ayala; however, the q^{1-n_a} vs. G_p straight line is employed instead of q^{1-n} vs. $G_p{}^*$. Equations (A.14) through (A.16) underlie the "modified Stumpf and Ayala method."

The analysis results of the modified Stumpf method for numerical examples are illustrated in Table 3(b), Table 6(b), and Figures 33–36.

Data Availability

The gas property data used for numerical simulation and filed application are generated by Londono and Hall-Yarborough correlations.

Conflicts of Interest

The authors declare that they have no known competing financial interests or personal relationships that could have appeared to influence the work reported in this paper.

Acknowledgments

This study has been supported by the Department of Middle East E&P and Department of Asia-Pacific E&P, Research Institute of Petroleum Exploration and Development, PetroChina. This work is supported by the National Science and Technology Major Project of China (Grant No. 2017ZX05030-003 and 2016ZX05015002).

References

[1] W. J. Lee and R. E. Sidle, "Gas reserves estimation in resource plays," in *Paper SPE-130102-MS presented at the SPE Unconventional Gas Conference*, Pittsburgh, Pennsylvania, 2010.

[2] J. Lee and R. Sidle, "Gas-reserves estimation in resource plays," *SPE Economics & Management*, vol. 2, no. 2, pp. 86–91, 2010.

[3] D. Denney, "Gas-reserves estimation in resource plays," *Journal of Petroleum Technology*, vol. 62, no. 12, pp. 65–67, 2010.

[4] R. E. Terry and J. B. Rogers, *Applied Petroleum Reservoir Engineering*, Pearson Education Inc, New Jersey, 3rd Edition edition, 2015.

[5] A. Satter and G. M. Iqbal, *Reservoir Engineering: The Fundamentals, Simulation, and Management of Conventional and Unconventional Recoveries*, Gulf Professional Publishing, Waltham, 2016.

[6] S. Okotie and B. Ikporo, *Reservoir Engineering: Fundamentals and Applications*, Springer Nature Switzerland AG, Switzerland, 2019.

[7] F. E. Gonzales, D. Ilk, and T. A. Blasingame, "A quadratic cumulative production model for the material balance of an abnormally pressured gas reservoir," in *Paper SPE-114044-MS presented at the SPE Western Regional and Pacific Section AAPG Joint Meeting*, Bakersfield, California, 2008.

[8] S. Moghadam, O. Jeje, and L. Mattar, "Advanced gas material balance in simplified format," *Journal of Canadian Petroleum Technology*, vol. 50, no. 1, pp. 90–98, 2011.

[9] N. Ezekwe, *Petroleum Reservoir Engineering Practice*, Pearson Education Inc, Boston, MA, 2011.

[10] J. Lee, J. B. Rollins, and J. P. Spivey, *Pressure Transient Testing*, Society of Petroleum Engineers, Richardson, TX, 2003.

[11] M. M. Kamal, *Transient Well Testing*, Society of Petroleum Engineers, Richardson, TX, 2009.

[12] J. P. Spivey and W. J. Lee, *Applied Well Test Interpretation*, Society of Petroleum Engineers, Richardson, TX, 2013.

[13] L. Mattar and D. M. Anderson, "A systematic and comprehensive methodology for advanced analysis of production data," in *Paper SPE-84472-MS presented at the SPE Annual Technical Conference and Exhibition*, Denver, Colorado, 2003.

[14] H. D. Sun, *Advanced Production Decline Analysis and Application*, Gulf Professional Publishing, Waltham, MA, 2015.

[15] H. Behmanesh, L. Mattar, J. M. Thompson, D. M. Anderson, D. W. Nakaska, and C. R. Clarkson, "Treatment of rate-transient analysis during boundary-dominated flow," *SPE Journal*, vol. 23, no. 4, pp. 1145–1165, 2018.

[16] J. J. Arps, "Analysis of decline curves," *Transactions of the AIME*, vol. 160, no. 1, pp. 228–247, 1945.

[17] M. J. Fetkovich, "Decline curve analysis using type curves," *Journal of Petroleum Technology*, vol. 32, no. 6, pp. 1065–1077, 1980.

[18] M. J. Fetkovich, M. E. Vienot, M. D. Bradley, and U. G. Kiesow, "Decline curve analysis using type curves: case histories," *SPE Formation Evaluation*, vol. 2, no. 4, pp. 637–656, 1987.

[19] R. D. Carter, "Characteristic behavior of finite radial and linear gas flow systems - constant terminal pressure case," in *Paper SPE-9887-MS presented at the SPE/DOE Low Permeability Gas Reservoirs Symposium*, Denver, Colorado, 1981.

[20] R. D. Carter, "Type curves for finite radial and linear gas-flow systems: constant-terminal-pressure case," *Society of Petroleum Engineers Journal*, vol. 25, no. 5, pp. 719–728, 1985.

[21] T. A. Blasingame, T. L. McCray, and W. J. Lee, "Decline curve analysis for variable pressure drop/variable flowrate systems," in *Paper SPE-21513-MS presented at the SPE Gas Technology Symposium*, Houston, Texas, 1991.

[22] J. C. Palacio and T. A. Blasingame, "Decline-curve analysis using type curves - analysis of gas well production data," in *Paper SPE-25909-MS presented at the SPE Rocky Mountain Regional/Low Permeability Reservoirs Symposium*, Denver, Colorado, 1993.

[23] T. A. Blasingame, J. L. Johnston, and W. J. Lee, "Type-curve analysis using the pressure integral method," in *Paper SPE-18799-MS presented at the SPE California Regional Meeting*, Bakersfield, California, 1989.

[24] R. G. Agarwal, D. C. Gardner, S. W. Kleinsteiber, and D. D. Fussell, "Analyzing well production data using combined type curve and decline curve analysis concepts," in *Paper SPE-49222-MS presented at the SPE Annual Technical Conference and Exhibition*, New Orleans, Louisiana, 1998.

[25] R. G. Agarwal, D. C. Gardner, S. W. Kleinsteiber, and D. D. Fussell, "Analyzing well production data using combined-type-curve and decline-curve analysis concepts," *SPE Reservoir Evaluation & Engineering*, vol. 2, no. 5, pp. 478–486, 1999.

[26] T. A. Blasingame and W. J. Lee, "Variable-rate reservoir limits testing," in *Paper SPE-15028-MS presented at the Permian Basin Oil and Gas Recovery Conference*, Midland, Texas, 1986.

[27] T. A. Blasingame and W. J. Lee, "Variable-rate reservoir limits testing of gas wells," in *Paper SPE-17708-MS presented at the SPE Gas Technology Symposium*, Dallas, Texas, 1988.

[28] L. X. Zhang, C. Q. Guo, Y. X. He, Y. Yu, and C. C. Liu, "Determination of gas in place for abnormally pressured gas reservoirs from production data," *Natural Gas Geoscience*, vol. 32, no. 5, pp. 703–717, 2021.

[29] L. Mattar and R. McNeil, "The "flowing" material balance procedure," in *Paper PETSOC-95-77 presented at the 46th Annual Technical Meeting of The Petroleum Society of CIM*, Banff in Alberta, 1995.

[30] L. Mattar and R. McNeil, "The "flowing" gas material balance," *Journal of Canadian Petroleum Technology*, vol. 37, no. 2, pp. 52–55, 1998.

[31] L. Mattar and D. Anderson, "Dynamic material balance (oil or gas-in-place without shut-ins)," in *Paper PETSOC-2005-113 presented at the 6th Canadian International Petroleum Conference*, Calgary, Alberta, 2005.

[32] L. Mattar, D. Anderson, and G. Stotts, "Dynamic material balance - oil-or gas-in-place without shut-ins," *Journal of Canadian Petroleum Technology*, vol. 45, no. 11, pp. 7–10, 2006.

[33] L. X. Zhang, Y. X. He, C. Q. Guo, and Y. Yu, "Dynamic material balance method for estimating gas in place of abnormally high-pressure gas reservoirs," *Lithosphere*, vol. 2021, no. - Special 1, article 6669012, 2021.

[34] P. Ye and L. F. Ayala, "A density-diffusivity approach for the unsteady state analysis of natural gas reservoirs," *Journal of Natural Gas Science and Engineering*, vol. 7, pp. 22–34, 2012.

[35] T. N. Stumpf and L. F. Ayala, "Rigorous and explicit determination of reserves and hyperbolic exponents in gas-well decline analysis," *SPE Journal*, vol. 21, no. 5, pp. 1843–1857, 2016.

[36] M. S. Alom, M. Tamim, and M. M. Rahman, "Decline curve analysis using rate normalized pseudo-cumulative function in a boundary dominated gas reservoir," *Journal of Petroleum Science and Engineering*, vol. 150, pp. 30–42, 2017.

[37] L. X. Zhang, C. Q. Guo, H. Jiang, G. Q. Cao, and P. Y. Chen, "Gas in place determination by material balance-quasipressure approximation condition method," *Acta Petrolei Sinica*, vol. 40, no. 3, pp. 337–349, 2019.

[38] Y. Wang and L. F. Ayala, "Explicit determination of reserves for variable-bottomhole-pressure conditions in gas rate-transient analysis," *SPE Journal*, vol. 25, no. 1, pp. 369–390, 2020.

[39] K. Jongkittinarukorn, N. Last, F. H. Escobar, and F. Srisuriyachai, "A straight-line DCA for a gas reservoir," *Journal of Petroleum Science and Engineering*, vol. 201, article 108452, 8 pages, 2021.

[40] J. Ansah, R. S. Knowles, and T. A. Blasingame, "A semi-analytic (p/z) rate-time relation for the analysis and prediction of gas well performance," in *Paper SPE-35268-MS presented at the SPE Mid-Continent Gas Symposium*, Amarillo, Texas, 1996.

[41] J. Ansah, R. S. Knowles, and T. A. Blasingame, "A semi-analytic (p/z) rate-time relation for the analysis and prediction of gas well performance," *SPE Reservoir Evaluation & Engineering*, vol. 3, no. 6, pp. 525–533, 2000.

[42] H. Y. Chen and L. W. Teufel, "Understanding the effects of reservoir and operating parameters on tight-gas production decline," in *Paper SPE-71066-MS presented at the SPE Rocky Mountain Petroleum Technology Conference*, pp. 1–10, Keystone, Colorado, 2001.

[43] H. Y. Chen and L. W. Teufel, "Estimating gas decline-exponent before decline-curve analysis," in *Paper SPE-75693-MS presented at the SPE Gas Technology Symposium*, Calgary, Alberta, Canada, 2002.

[44] R. P. Sutton, "Fundamental PVT calculations for associated and gas-condensate natural gas systems," in *Paper SPE-97099-MS presented at the SPE Annual Technical Conference and Exhibition*, Dallas, Texas, 2005.

[45] R. P. Sutton, "Fundamental PVT calculations for associated and gas/condensate natural-gas systems," *SPE Reservoir Evaluation & Engineering*, vol. 10, no. 3, pp. 270–284, 2007.

[46] K. R. Hall and L. Yarborough, "A new equation of state for Z-factor calculations," *Oil and Gas Journal*, vol. 71, no. 25, pp. 82–85, 1973.

[47] F. E. Londono, R. A. Archer, and T. A. Blasingame, "Simplified correlations for hydrocarbon gas viscosity and gas density - validation and correlation of behavior using a large-scale database," in *Paper SPE-75721-MS presented at the SPE Gas Technology Symposium*, Calgary, Alberta, 2002.

[48] F. E. Londono, R. A. Archer, and T. A. Blasingame, "Correlations for hydrocarbon gas viscosity and gas density - validation and correlation of behavior using a large-scale database," *SPE Reservoir Evaluation & Engineering*, vol. 8, no. 6, pp. 561–572, 2005.

[49] M. L. Fraim and R. A. Wattenbarger, "Gas reservoir decline-curve analysis using type curves with real gas pseudopressure and normalized time," *SPE Formation Evaluation*, vol. 2, no. 4, pp. 671–682, 1987.